JOURNAL OF GUIDANCE, CONTROL, AND DYNAMICS
Vol. 32, No. 4, July–August 2009

Nonlinear Robust Stochastic Control for Unmanned Aerial Vehicles

Yunjun Xu*
University of Central Florida, Orlando, Florida 32816

DOI: 10.2514/1.40753

Almost all dynamical systems experience inherent uncertainties such as environmental disturbance, sensor noise, and modeling error due to approximations. In safety-critical applications, such as control of unmanned aerial vehicles, characterizing and controlling the statistical performance of the system become important tasks. This paper describes a new robust stochastic control methodology that is capable of controlling the statistical nature of state or output variables of a nonlinear system to desired (attainable) statistical properties (e.g., moments). First, as the online step, an asymptotically stable and robust output tracking controller is designed in which discontinuous functions are not involved. Second, as the offline step, undetermined control parameters in the closed-loop system are optimized through nonlinear programming. In this constrained optimization, the error between the desired and actual moments of state or output variables is minimized subject to constraints on statistical moments. As the key point to overcome the difficulties in solving the associated Fokker–Planck equation, a direct quadrature method of moments is proposed. In this approach, the state probability density function is expressed in terms of a finite collection of Dirac delta functions, with the associated weights and locations determined by moment equations. The advantages of the proposed method are 1) the ability to control any specified stationary moments of the states or output probability density function, 2) no need for the state process to be a Gaussian, and 3) robustness with respect to parametric and functional uncertainties. An unmanned aerial vehicle command-tracking control is used to demonstrate the capability of the proposed nonlinear stochastic control method and the results are successfully validated by Monte Carlo simulations.

Nomenclature

C_{D0}	=	zero-lift drag coefficient
$\boldsymbol{B}$	=	$[b_{ij}]$, input matrix, $i = 1, \ldots, n$ and $j = 1, \ldots, m$
$\boldsymbol{D}$	=	$[D_{ij}]$, uncertainty bound of the input matrix, $i = 1, \ldots, p$ and $j = 1, \ldots, p$
D_{drag}	=	drag
$d\beta_j$	=	normal distribution, $j = 1, \ldots, N_w$
$\boldsymbol{E}$	=	$[E_{ij}]$, diffusion term in the Fokker–Planck equation, $i = 1, \ldots, N_s$ and $j = 1, \ldots, N_s$
e_i	=	error signal, $i = 1, \ldots, p$
$\boldsymbol{F}$	=	$[F_i]$, uncertainty bound of the state dynamics, $i = 1, \ldots, p$
$\boldsymbol{f}$	=	$[f_i]$, state function, $i = 1, \ldots, n$
$\boldsymbol{G}$	=	$[g_{ij}]$, additive noise associated input matrix, $i = 1, \ldots, n$ and $j = 1, \ldots, N_w$
g	=	gravitational coefficient
$\boldsymbol{h}$	=	$[h_i]$, output function, $i = 1, \ldots, p$
$\boldsymbol{I}$	=	identity matrix with a proper dimension
k	=	induced drag coefficient
k_i	=	moment index for state i, $i = 1, \ldots, N_s$
k_n	=	load-factor coefficient
L	=	Lie derivative operator
$M^{k_1,\ldots,k_{N_s}}$	=	$k_1, k_2, \ldots, k_{N_s}$ moment of the state probability density function
m	=	number of control variables
N	=	number of nodes in the direct quadrature form
N_s	=	number of state variables in the Itô form
N_w	=	number of additive noise
n	=	number of states
n_g	=	load factor of the unmanned aerial vehicle
p	=	$p(\boldsymbol{x})$, probability density function
p	=	number of output variables
$\boldsymbol{Q}$	=	$[Q_{ij}]$, covariance matrix
$\boldsymbol{r}$	=	$[r_i]$, relative degree of the output variable, $i = 1, \ldots, p$
S	=	wing area of the unmanned aerial vehicle
$\boldsymbol{s}$	=	$[s_i]$, sliding manifold, $i = 1, \ldots, p$
$\bar{S}_{k_1,\ldots,k_{N_s}}$	=	$k_1, k_2, \ldots, k_{N_s}$ moment constraint
T	=	thrust
t	=	time
U	=	mean wind speed
$\boldsymbol{u}$	=	$[u_j]$, control variables, $j = 1, \ldots, m$
V	=	airspeed
V_w	=	wind speed
W	=	weight of the unmanned aerial vehicle
$\boldsymbol{w}$	=	$[w_j]$, Weiner process, $j = 1, \ldots, N_w$
w_α	=	weight for abscissas, $\alpha = 1, \ldots, N$
x_i	=	state variable, $i = 1, \ldots, n$
$\widehat{x}_j$	=	state variables in the Itô form, $j = 1, \ldots, N_s$
$\langle \widehat{x}_j \rangle_\alpha$	=	property vector of node α for state j, abscissas
$\boldsymbol{y}$	=	$[y_i]$ output variable, $i = 1, \ldots, p$
z	=	altitude
γ	=	flight-path angle
$\boldsymbol{\Delta}$	=	$[\Delta_{ij}]$, uncertainty of the input matrix, $i = 1, \ldots, p$ and $j = 1, \ldots, p$
δ	=	Dirac delta function
$\zeta_{j\alpha}$	=	weighted abscissas, $j = 1, \ldots, N_s$ and $\alpha = 1, \ldots, N$
$\boldsymbol{\eta}$	=	$[\eta_i]$, control parameters, $i = 1, \ldots, p$
$\boldsymbol{\lambda}$	=	$[\lambda_{k,i}]$, control parameters, $k = 0, \ldots, r_i - 2$ and $i = 1, \ldots, p$
μ	=	mean value
$\boldsymbol{\xi}$	=	$[\xi_i]$, control parameters, $i = 1, \ldots, p$
ρ	=	atmospheric density
σ	=	standard deviation
ϕ	=	bank angle
χ	=	heading angle

Received 2 September 2008; revision received 19 November 2008; accepted for publication 1 March 2009.

*Assistant Professor, Department of Mechanical, Materials, and Aerospace Engineering; yunjunxu@mail.ucf.edu.

Subscripts

a	=	actual value
c	=	command
d	=	desired signal
max	=	maximum value
min	=	minimum value
0	=	initial condition

Superscripts

l	=	lth derivative
T	=	matrix transpose
$\hat{}$	=	nominal information
$\bar{}$	=	variables or functions defined in the Itô form
$+$	=	pseudoinverse

I. Introduction

VIEWING system behaviors within a stochastic framework allows for the inclusion of random disturbances and calculation of expected long-term system trends. However, controlling a stochastic system is more challenging as compared with its deterministic counterpart, because the controller should be designed to achieve not only the desired characteristics typically required by deterministic systems, but also desired statistical characteristics (e.g., user-specified variances, covariance, and/or higher-order moments).

Normally, Monte Carlo simulation approaches are used to find proper control parameters such that a desired statistical distribution of the closed-loop system performance can be achieved. However, this approach has a polynomial complexity in computation [1]. It will become intractable when the system is large, which may result in a prohibitive number of control design iterations and CPU and labor time. Furthermore, due to the stochastic nature of the random number generation, results may vary for each of the design iterations.

To reduce the computational cost and provide a systematic design methodology, extensive research efforts were spent for both linear and nonlinear stochastic systems, as discussed subsequently.

On one hand, the stochastic control for linear systems (such as linear quadratic Gaussian (LQG), observer-based covariance control, optimal sliding mode regulator, and minimum energy covariance control, etc.) has been well studied [2–12]. On the other hand, the methods have been investigated to address nonlinear stochastic problems, which can be broadly put into three categories.

The first and the most intuitive way of handling nonlinear stochastic control problems is to linearize the system in a statistical way, after which linear stochastic control methods could be applied [13]. The shortcoming of this method is obvious: it is expected that a linear controller will only provide a good closed-loop performance locally (i.e., close to set points for nonlinear systems [14]).

The second approach to solve nonlinear stochastic control problems is via the solution of the associated Fokker–Planck equation (FPE) once the structure of the closed-loop system is known. However, solving the associated FPE [15–17] makes this problem cumbersome with few exceptions, due to the curse of dimensionality [18–21]. To mitigate the computational cost, methods such as the path integral method [22], cell-mapping method [23], and adaptive grid methods [24,25] have been tried. However, the computational cost in these methodologies is still high even for low-dimension nonlinear control problems.

Much research has been conducted in the third category, approximation methods [14,26–32], through which the solution of the FPE is approximated. For example, the Gaussian closure method investigated by Sun and Xu [32] is one of them. In this approach, the moments of order higher than two are approximated in terms of the first- and second-order moments. However, the expectation of nonlinear terms has to be integrated over a domain big enough such that the majority of the probability can be captured. In the approach proposed by Sobczy et al. [27], Wojtkiewicz and Bergman [14], and Yue and Wang [33], a maximum entropy method has been applied; thus, a system of nonlinear equations can be formed for user-specified response moments. The availability of the response probability density function (PDF) makes the evaluation of higher-order response moments fairly effective, even though the PDF is approximated. In the paper by Chang et al. [28], describing functions were applied to study the covariance control for a nonlinear system. Kim and Rock [29] used dual properties in designing a suboptimal stochastic control in which the feedback control structure is predefined and the mean value of the performance is controlled. However, the weighting matrix for the error covariance needs to be diagonal and no equality or inequality constraints can be included. Forbes et al. [30] used Gram–Charlier expansions as the PDF basis functions and obtained an approximately parameterized response PDF to track the target PDF in steady state, though without a guaranteed stability. Su and Strunz [31] applied the polynomial-chaos-based average method to identify the uncertainty propagation of the 12-pulse diode rectifier in aircraft power systems; yet this method can only consider the case with one noise resource, because the expansion series vary for different types of noise. Kumar et al. [34] applied the Galerkin projection method in solving the associated FPE for a particular unconstrained nonlinear optimal control problem based on the policy iteration algorithm.

In short, most of the methods mentioned previously have one or several of the following limitations:

1) It is difficult to solve the FPE in general.

2) Some expectations of nonlinear terms cannot be obtained effectively.

3) It is not easy to handle inequality and equality constraints.

4) Stability is not guaranteed.

In the present work, a novel approach is proposed, referred to as the direct quadrature method of moments (DQMOM), along with an asymptotically stable nonlinear tracking control. This approach involves representing the state PDF in terms of a finite summation of Dirac delta functions, for which the weights and locations (abscissas) are determined based on moments constraints. Using a small number of scalars, the method is able to efficiently and accurately model stochastic processes described by the multidimensional FPE through a set of ordinary differential equations (ODEs). Together with the DQMOM approach, a nonlinear controller is designed here based on the concepts of sliding manifold and input–output feedback linearization with guaranteed asymptotic tracking stability. Different from the commonly used sliding mode control (SMC) [35–44], the high-speed switching (discontinuous) function shown in typical SMCs or higher-order SMCs has been removed to satisfy the continuity requirement in the partial derivatives of the associated FPE. In addition, the inherent chattering problem experienced in the commonly used SMC can be eliminated.

The main contributions of the paper can be summarized as follows. First, the existence of a finite moment index implies that the controlled system is stable up to the highest order of statistical moments included in the offline design. Second, selected moments of the state or output variables can be controlled accurately in steady state and the state process does not need to be a Gaussian. Third, the nonlinear controller proposed here is asymptotically stable and robust to bounded parametric as well as functional uncertainties.

The rest of this paper is organized as follows. First, the system model of an affine nonlinear stochastic system is described along with the control objectives and the nominal system used in the design stage. Second, the governing equations of the weights and abscissas, which are used in representing the state PDF, are derived for the FPE based upon the proposed quadrature-based moment approach. Third, a nonlinear robust control method is proposed based on the concepts of input–output feedback linearization and sliding manifold without involving discontinuous functions. Next, the undetermined control parameters, weights, and abscissas are optimized offline through a constrained nonlinear optimization. Finally, a nontrivial numerical example is illustrated, followed by the conclusion. To make the presentation clear, detailed theoretical proofs are given in Appendices A, B, and C.

II. System Model and Control Objectives

Let us consider the following control-affine nonlinear stochastic differential equation (SDE) with additive noise:

$$x_i^{(l_i)} = f_i(\boldsymbol{x}_1, \ldots, \boldsymbol{x}_n, t) + \sum_{j=1}^{m} b_{ij}(\boldsymbol{x}_1, \ldots, \boldsymbol{x}_n)u_j + \sum_{j=1}^{N_w} g_{ij}(\boldsymbol{x}_1, \ldots, \boldsymbol{x}_n)w_j(t), \qquad i = 1, \ldots, n \tag{1}$$

and an output model to be

$$y_i = h_i(\boldsymbol{x}_1, \ldots, \boldsymbol{x}_n), \qquad i = 1, \ldots, p \tag{2}$$

where $\boldsymbol{x}_i = [x_i, \dot{x}_i, \ldots, x_i^{(l_i-1)}]^T \in \Re^{l_i}$ and $x_i^{(l_i-1)} \triangleq d^{l_i-1}x_i/dt^{l_i-1}$ are states with up to $l_i - 1$ derivatives, $\boldsymbol{u} = [u_1, \ldots, u_m]^T \in \Re^m$ is the control input, and $\boldsymbol{B} = [b_{ij}(\boldsymbol{x}_1, \ldots, \boldsymbol{x}_n)] \in \Re^{n\times m}$ and $\boldsymbol{f} = [f_1, \ldots, f_n]^T \in \Re^n$ are the input matrix and state function, respectively. The relative degree of the output $\boldsymbol{y} = \boldsymbol{h} = [y_1, \ldots, y_p]^T \in \Re^p$ is $\boldsymbol{r} = [r_1, \ldots, r_p]^T \in \Re^p$. In this paper, only the case when $p \le m$ is considered to avoid numerical errors in the pseudoinverse associated with the proposed controller. When $p > m$, singular perturbation or multi-time-scale decomposition methods can be used [45,46]. Also, $\boldsymbol{w}(t) = [w_1, \ldots, w_{N_w}] \in \Re^{N_w}$ is assumed to be a Weiner process [15] with a zero mean and a covariance matrix of $\boldsymbol{Q}(t)$, and $\boldsymbol{G} = [g_{ij}] \in \Re^{n\times N_w}$ is the associated matrix.

The nonlinear robust controller is designed based on the following nominal system,

$$x_i^{(l_i)} = \hat{f}_i(\boldsymbol{x}_1, \ldots, \boldsymbol{x}_n, t) + \sum_{j=1}^{m} \hat{b}_{ij}(\boldsymbol{x}_1, \ldots, \mathbf{x}_n)u_j, \quad i = 1, \ldots, n \tag{3}$$

with the nominal output model as

$$y_i = \hat{h}_i(\boldsymbol{x}_1, \ldots, \boldsymbol{x}_n), \qquad i = 1, \ldots, p \tag{4}$$

where $\hat{}$ represents the nominal information. The parametric uncertainties of the input matrix are bounded by $|\Delta_{ij}| \le D_{ij}$ $(i, j = 1, \ldots, p)$, where the bounds are calculated by

$$(\boldsymbol{I} + \boldsymbol{\Delta}) = [L_{\boldsymbol{B}}L_f^{r-1}\boldsymbol{h}(\boldsymbol{x})][L_{\hat{\boldsymbol{B}}}L_{\hat{f}}^{r-1}\hat{\boldsymbol{h}}(\boldsymbol{x})]^+, \qquad \boldsymbol{\Delta} \in \Re^{p\times p} \tag{5}$$

and $\boldsymbol{I}$ is an identity matrix with a proper dimension, $\boldsymbol{B}$ and $\hat{\boldsymbol{B}}$ are assumed to satisfy the matching condition [41] [that is, the maximum eigenvalue of the matrix $\boldsymbol{D}$ satisfy $\lambda_{\max}(\boldsymbol{D}) < 1$], and L and $+$ are used to denote the Lie derivative and the pseudoinverse, respectively. The error between the nominal and actual state functions is bounded by $\boldsymbol{F} = [F_1, \ldots, F_p]^T \in \Re^p$ as

$$F_i = |-L_f^{r_i}h_i + L_{\hat{f}}^{r_i}\hat{h}_i|, \qquad i = 1, \ldots, p \tag{6}$$

Note that the particular form of these uncertainties is coming from the stability proof of the output tracking control design.

The control objectives are 1) to stabilize the system while being capable of tracking the desired trajectory $y_{i,d}$, where $i = 1, \ldots, p$, and 2) to achieve desired stationary statistics of the states/output PDF. For example, the desired stationary PDF distribution can be characterized by, but not limited to, the values of mean, variance, and any high-order moments.

III. Nonlinear Stochastic Control Based upon DQMOM

Once the feedback control law $u_j = u_j(\boldsymbol{x}_1, \ldots, \boldsymbol{x}_n, \boldsymbol{\lambda}, \boldsymbol{\eta})$, to be described in the next section, is designed, the state equation of the closed-loop SDE (1) can be rewritten as

$$x_i^{(l_i)} = f_i(\boldsymbol{x}_1, \ldots, \boldsymbol{x}_n, t) + \sum_{j=1}^{m} b_{ij}(\boldsymbol{x}_1, \ldots, \boldsymbol{x}_n)u_j(\boldsymbol{x}_1, \ldots, \boldsymbol{x}_n, \boldsymbol{\lambda}, \boldsymbol{\eta}) + \sum_{j=1}^{N_w} g_{ij}(\boldsymbol{x}_1, \ldots, \boldsymbol{x}_n)w_j(t), \qquad i = 1, \ldots, n \tag{7}$$

where $\boldsymbol{\lambda}$ and $\boldsymbol{\eta}$ are the control parameters to be determined. The l_ith-order ODE (7) can be converted into the Itô form as

$$d\widehat{x}_i = \widehat{f}_i(\boldsymbol{x}_1, \ldots, \boldsymbol{x}_n, \boldsymbol{\lambda}, \boldsymbol{\eta}, t)dt + \sum_{j=1}^{N_w} \widehat{g}_{ij}(\boldsymbol{x}_1, \ldots, \boldsymbol{x}_n)d\beta_j(t), \qquad i = 1, \ldots, N_s \tag{8}$$

where

$$N_s = \sum_{i}^{n} l_i$$

is the number of states $\widehat{x}_i$ (i.e., $\widehat{\boldsymbol{x}}(t) = [\widehat{x}_i] \in \Re^{N_s}$) in the first-order system. According to Jazwinski [15], $w_j(t) \sim d\beta_j(t)/dt$ and $d\beta_j(t) \sim \mathbb{N}(0, dt)$ is a normal distribution. $\widehat{\boldsymbol{G}} = [\widehat{g}_{ij}] \in \Re^{N_s\times N_w}$ is the associated matrix. Note that Eq. (7) is preferred in the nonlinear robust control design, whereas Eq. (8) is more convenient for the stochastic part.

If the process described by the SDE (8) is a Markovian diffusion process, the PDF characterizing this process is governed by the FPE [15–17] as

$$\frac{\partial p}{\partial t} = -\sum_{i=1}^{N_s} \frac{\partial[p\widehat{f}_i]}{\partial \widehat{x}_i} + \frac{1}{2}\sum_{i=1}^{N_s}\sum_{j=1}^{N_s} \frac{\partial^2[p(\widehat{\boldsymbol{G}}\boldsymbol{Q}\widehat{\boldsymbol{G}}^T)_{ij}]}{\partial \widehat{x}_i \partial \widehat{x}_j} \tag{9}$$

where $p = p(\widehat{\boldsymbol{x}})$ is the state PDF. The first term on the right-hand side (RHS) of the FPE is the drift term, whereas the second one is the diffusion term.

Here, a new quadrature-based moment approach is proposed for solving the FPE efficiently. This method involves the approximation of the state PDF in terms of a finite summation of Dirac delta functions as

$$p(\widehat{\boldsymbol{x}}(t)) = \sum_{\alpha=1}^{N} w_\alpha(t) \prod_{j=1}^{N_s} \delta[\widehat{x}_j - \langle \widehat{x}_j \rangle_\alpha] \tag{10}$$

where N is the number of nodes, $w_\alpha = w_\alpha(t)$ denotes the corresponding weight for node α $(\alpha = 1, \ldots, N)$, and $\langle \widehat{x}_j \rangle_\alpha = \langle \widehat{x}_j \rangle_\alpha(t)$ $(j = 1, \ldots, N_s)$ represents the property vector of node α, called *abscissas* here.

Theorem 1: The dynamics of the abscissas $\langle \widehat{x}_j \rangle_\alpha$ and weights w_α are governed by the following differential algebraic equations:

$$\sum_{\alpha=1}^{N}\left[\left(1 - \sum_{j=1}^{N_s} k_j\right)\prod_{q=1}^{N_s}\langle \widehat{x}_q \rangle_\alpha^{k_q}\right]a_\alpha + \sum_{\alpha=1}^{N}\sum_{j=1}^{N_s} k_j \langle \widehat{x}_j \rangle_\alpha^{k_j-1} \prod_{q=1, q\ne j}^{N_s} \langle \widehat{x}_q \rangle_\alpha^{k_q} c_{j\alpha} = \bar{S}_{k_1,\ldots,k_{N_s}} \tag{11}$$

where

$$dw_\alpha/dt \triangleq a_\alpha, \qquad \alpha = 1, \ldots, N \tag{12}$$

and

$$d\zeta_{j\alpha}/dt \triangleq c_{j\alpha}, \qquad j = 1, \ldots, N_s, \qquad \alpha = 1, \ldots, N \tag{13}$$

Here, the weighted abscissas $\zeta_{j\alpha} \triangleq w_\alpha \langle \widehat{x}_j \rangle_\alpha$ is introduced. The $k_1, k_2, \ldots, k_{N_s}$ moment constraint is derived as

$$\bar{S}_{k_1,\ldots,k_{N_s}} \triangleq \bar{S}^1_{k_1,\ldots,k_{N_s}} + \bar{S}^2_{k_1,\ldots,k_{N_s}}$$

where

$$\bar{S}^{1}_{k_1,\ldots,k_{N_s}} = \sum_{i=1}^{N_s}\sum_{\alpha=1}^{N} k_i w_\alpha(t)\langle\widehat{x}_1\rangle_\alpha^{k_1}\cdots\langle\widehat{x}_{i-1}\rangle_\alpha^{k_{i-1}}\langle\widehat{x}_i\rangle_\alpha^{k_i-1}\langle\widehat{x}_{i+1}\rangle_\alpha^{k_{i+1}}\cdots \langle\widehat{x}_{N_s}\rangle_\alpha^{k_{N_s}}\widehat{f}_i(\langle\widehat{x}_1\rangle_\alpha,\ldots,\langle\widehat{x}_{N_s}\rangle_\alpha) \tag{14}$$

and

$$\bar{S}^{2}_{k_1,\ldots,k_{N_s}} = \begin{cases} \sum_{i=1}^{N_s}\sum_{j=1}^{N_s}\sum_{\alpha=1}^{N} w_\alpha k_i k_j\left(\prod_{q=1}^{N_s}\langle\widehat{x}_q\rangle_\alpha^{k_q}\right)\Big/\langle\widehat{x}_i\rangle_\alpha\langle\widehat{x}_j\rangle_\alpha[\boldsymbol{E}(\widehat{\boldsymbol{x}})]_{ij}\big|_{\langle\widehat{x}_1\rangle_\alpha,\ldots,\langle\widehat{x}_{N_s}\rangle_\alpha} & i\neq j \\ \sum_{i=1}^{N_s}\sum_{i=1}^{N_s}\sum_{\alpha=1}^{N} w_\alpha k_i(k_i-1)\left(\prod_{q=1}^{N_s}\langle\widehat{x}_q\rangle_\alpha^{k_q}\right)\Big/\langle\widehat{x}_i\rangle_\alpha^2[\boldsymbol{E}(\widehat{\boldsymbol{x}})]_{ii}\big|_{\langle\widehat{x}_1\rangle_\alpha,\ldots,\langle\widehat{x}_{N_s}\rangle_\alpha} & i=j \end{cases} \tag{15}$$

where $\boldsymbol{E}\triangleq\frac{1}{2}\widehat{\boldsymbol{G}}\boldsymbol{Q}\widehat{\boldsymbol{G}}^T$ is the diffusion term. The proof of Theorem 1 is shown in Appendix A. Once the abscissas and weights are calculated, any selected statistical moment of the state PDF can be found from

$$M^{k_1k_2,\ldots,k_{N_s}} \triangleq \sum_{\alpha=1}^{N} w_\alpha\prod_{j=1}^{N_s}\langle\widehat{x}_j\rangle_\alpha^{k_j} \tag{16}$$

where $k_1, k_2, \ldots, k_{N_s}$ are nonnegative integers and used to denote the $k_1, k_2, \ldots, k_{N_s}$ moments of the state statistics.

Lemma 1: For any selected nonnegative integers $k_1, k_2, \ldots, k_{N_s}$, the corresponding stationary moment of the PDF is governed by

$$\bar{S}_{k_1,\ldots,k_{N_s}} = 0 \tag{17}$$

Proof: In steady state, the abscissas and weights of the moments will not change in time; therefore, based on Eq. (11), the left-hand side (LHS) is zero.

Through the approach described in Theorem 1 and Lemma 1, weights and abscissas are determined based on the constraints from the evolution of moments. Using a small number of scalars, this method is able to efficiently and accurately model stochastic processes described by the multivariable FPE through a set of ODEs instead of computationally intensive partial differential equations.

IV. Nonlinear Robust Control

In this section, a nonlinear robust controller $u_j = u_j(\boldsymbol{x}_1, \ldots, \boldsymbol{x}_n, \boldsymbol{\lambda}, \boldsymbol{\eta})$ will be proposed. Unlike a commonly used SMC approach [35–37], there is no discontinuous function involved. The latter fact is preferred by the FPE-based approach because of continuity requirements in the partial derivatives. Let us define the sliding manifold $\boldsymbol{s} = [s_1, \ldots, s_p]^T \in \Re^p$ as

$$s_i = \sum_{k=0}^{r_i-2}\lambda_{k,i}e_i^{(k)} + e_i^{(r_i-1)}, \qquad i = 1, \ldots, p \tag{18}$$

where $\lambda_{k,i} > 0$ ($k = 0, \ldots, r_i - 2$ and $i = 1, \ldots, p$) can be any positive number and the error signal is defined as $e_i = y_{i,d} - y_i$ ($i = 1, \ldots, p$).

Theorem 2: For a nonlinear system [Eq. (1)] with bounded parametric and functional uncertainties [Eqs. (5) and (6)], the proposed multiple-input/multiple-output feedback control scheme

$$\boldsymbol{u} = [L_{\hat{\boldsymbol{B}}}L_{\hat{f}}^{r-1}\hat{\boldsymbol{h}}(\boldsymbol{x})]^{+}\left[\frac{d^r\boldsymbol{y}_d}{dt^r} - L_{\hat{f}}^{r}\hat{\boldsymbol{h}}(\boldsymbol{x}) + \sum_{k=0}^{r-2}\boldsymbol{\lambda}_k\cdot\boldsymbol{e}^{(k+1)} + \boldsymbol{\xi}\cdot\boldsymbol{s}\right] \tag{19}$$

guarantees that the closed-loop system is globally asymptotically stable for tracking desired signal $y_{i,d}$. Note that $\boldsymbol{\lambda}_k = [\lambda_{k,i}]$ ($i = 1, \ldots, p$) and the elementwise multiplication $\boldsymbol{\xi}\cdot\boldsymbol{s} = [\xi_1 s_1, \ldots, \xi_p s_p]^T \in \Re^p$ is applied.

Lemma 2: The time-varying feedback gain $\boldsymbol{\xi} = [\xi_1, \ldots, \xi_p]^T \in \Re^p$ can be uniquely solved from

$$\boldsymbol{F} + \boldsymbol{D}\left|\frac{d^r\boldsymbol{y}_d}{dt^r} - L_{\hat{f}}^{r}\hat{\boldsymbol{h}}(\boldsymbol{x}) + \sum_{k=0}^{r-2}\boldsymbol{\lambda}_k\cdot\boldsymbol{e}^{(k+1)}\right| + \boldsymbol{\eta}\cdot\boldsymbol{s} = (\boldsymbol{I}-\boldsymbol{D})\boldsymbol{\xi}\cdot\boldsymbol{s} \tag{20}$$

for any positive numbers $\boldsymbol{\lambda}$ and $\boldsymbol{\eta}$. In the case of $s_i \to 0$, the magnitude of $\xi_i s_i$ instead of ξ_i will be calculated using Eq. (20), because the proposed controller [Eq. (19)] only uses $\xi_i s_i$. The sign of $\xi_i s_i$ is determined by s_i because $\xi_i > 0$. The proofs of Theorem 2 and Lemma 2 are provided in Appendices B and C, respectively.

V. Offline Constrained Nonlinear Optimization

The objective is to achieve the desired moments of the closed-loop system. The basic procedure involves the minimization of the weighted error norm between the desired moment $M_d^{k_1k_2,\ldots,k_{N_s}}$ and actual moment $M^{k_1k_2,\ldots,k_{N_s}}$ through nonlinear programming (one of the two objectives for the stochastic control design). The equality constraint is

$$\sum_{\alpha=1}^{N} w_\alpha = 1$$

(property of the PDF) and Eq. (17) (a set of nonlinear functions), and $\boldsymbol{\eta} > 0$ (stability requirement), $\boldsymbol{\lambda} > 0$ (stability requirement), and $w_\alpha > 0$ (property of the PDF) are inequality constraints. The parameters to be optimized are control parameters $\boldsymbol{\lambda}$ and $\boldsymbol{\eta}$, the weights w_α, and the abscissas $\langle\widehat{x}_j\rangle_\alpha$. Note that due to the flexibility of the nonlinear programming (NLP) approach used here, the performance index can be extended to a more general form, but not limited to the quadratic-type index.

The structure of the optimization is summarized and demonstrated, as shown in Fig. 1. First, the desired stationary moments $M_d^{k_1k_2,\ldots,k_{N_s}}$ are specified by users. After that, an NLP optimal control algorithm will be used to find desired optimal control parameters $\boldsymbol{\lambda}$ and $\boldsymbol{\eta}$ through the DQMOM approach. Finally, the found controller parameters will be implemented in the nonlinear robust control. In brief, the algorithm is outlined here:

Step 1) Design nonlinear robust control using Theorem 2 and Lemma 2.

Step 2) Reformulate the closed-loop system in the Itô form including the unknown but constrained control parameters.

Step 3) From the Itô form, construct the governing equation of the state probability density using the proposed DQMOM approach based on Theorem 1 and Lemma 1.

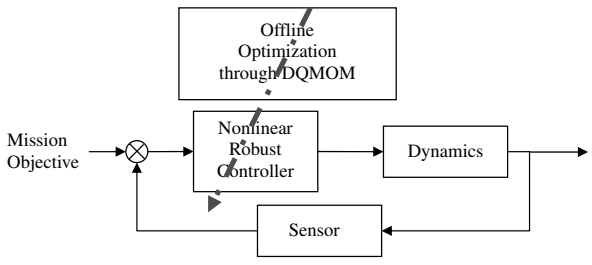

Fig. 1 Outline of the stochastic robust control algorithm.

Step 4) Form a nonlinear programming problem to solve the unknown control parameters as described in this section.

Step 5) Apply the found control parameters in the nonlinear robust controller and the statistic performance can be validated through Monte Carlo simulation.

VI. Numerical Simulation

The effectiveness of the proposed algorithm is demonstrated in the following nontrivial generic unmanned aerial vehicle (UAV) command-tracking problem. Note that although the example used here is a state feedback controller, the methodologies proposed in this paper can be extended to output feedback control, in which the actual and desired moments of output variables instead of state variables will be in the offline optimization.

A. Dynamics Model and Control Objectives

Assuming that the Earth is flat and the fuel expenditure is negligible (i.e., the center of mass is time-invariant), the UAV dynamics can be expressed in the wind system as

$$\dot{\boldsymbol{x}} = \begin{bmatrix} \dot{V} \\ \dot{\gamma} \\ \dot{\chi} \end{bmatrix} = \begin{bmatrix} g[(T - D_{\text{drag}})/W - \sin\gamma] \\ (g/V)(k_n n_g \cos\phi - \cos\gamma) \\ g k_n n_g \sin\phi/(V\cos\gamma) \end{bmatrix} + \boldsymbol{G}\boldsymbol{w} \tag{21}$$

where the drag is calculated by

$$D_{\text{drag}} = 0.5\rho(V - V_w)^2 S C_{D0} + 2kk_n^2 n_g^2 W^2/[\rho(V - V_w)^2 S] \triangleq D_{\text{drag},1} + D_{\text{drag},2} \tag{22}$$

Here, V, γ, and χ represent the airspeed, flight-path angle, and heading angle, respectively. The control variables are the applied thrust T ($T \le 113,868.8N$), load factor n_g ($-1 \le n_g \le 2.66$), and bank angle ϕ ($-25\,\text{deg} \le \mu \le 25\,\text{deg}$). The constants used in the model [47] are wing area $S = 37.16\ \text{m}^2$, zero-lift drag coefficient $C_{D0} = 0.02$, load-factor effectiveness $k_n = 1$, induced drag coefficient $k = 0.1$, gravitational coefficient $g = 9.81\ \text{kg/m}^2$, atmospheric density $\rho = 1.2207\ \text{kg/m}^3$, and the weight of the selected UAV $W = 14515$ g. To facilitate the control design, the drag has been separated into two parts:

$$D_{\text{drag},1} \triangleq 0.5\rho(V - V_w)^2 S C_{D0}$$

and

$$D_{\text{drag},2} \triangleq 2kk_n^2 n_g^2 W^2/[\rho(V - V_w)^2 S]$$

as shown in Eq. (22). The gust model $V_w = V_{w,\text{normal}} + V_{w,\text{tang}}$ is scaled based on [48] and varies according to the altitude z. In the simulated gust, the normal wind shear is given by

$$V_{w,\text{normal}} = 0.215U\log_{10}(z) + 0.285U \tag{23}$$

where $U = 22.07$ m/s is the mean wind speed at an altitude of 5000 m. The turbulence part of the wind gust $V_{w,\text{tang}}$ has a Gaussian distribution with a zero mean and a standard derivation of $0.09U$.

The first control objective is to track the desired output $V_d =$ 90 m/s, $\gamma_d = 5$ deg, and $\chi_d = 1$ deg from the initial condition of $V_0 = 80$ m/s, $\gamma_0 = 0$ deg, and $\chi_0 = 0$ deg. The second objective is to achieve desired stationary performance statistics of the state variables under two different noise levels. Here, a quadratic form of the index is used as

$$J = \left[\sum_{i=1}^{3} \varpi_i(\mu_i - \mu_{i,d})^2 + \sum_{i=1}^{3} \vartheta_i(\sigma_i^2 - \sigma_{i,d}^2)^2\right]^{1/2} \tag{24}$$

where the mean μ_i ($i = 1, 2, 3$) and variance σ_i^2 ($i = 1, 2, 3$) variables can be calculated from the moments [Eq. (16)]. The weights of the performance index (i.e., ϖ_i and ϑ_i, where $i = 1, 2, 3$) are tuned to achieve a better convergence in NLP.

B. Uncertainty and Noise Models

The uncertainties and noise considered in the control design and simulation in Sec. VI.E are described here. In this problem, $\boldsymbol{w}(t) \in \Re^3$ [Eq. (21)] is assumed to be a Weiner process with a zero mean and a covariance matrix of $\boldsymbol{Q}(t)$, and the associated matrix $\boldsymbol{G}$ is assumed to be the identity matrix as $\boldsymbol{I} \in \Re^{3\times 3}$. For the purpose of illustrating the capabilities of the algorithm, two noise settings are tried:

$$\text{case 1: } \boldsymbol{Q} = \begin{bmatrix} (0.25\ \text{m/s}^2)^2 & 0 & 0 \\ 0 & (1\,\text{deg/s})^2 & 0 \\ 0 & 0 & (1\,\text{deg/s})^2 \end{bmatrix} \tag{25}$$

and

$$\text{case 2: } \boldsymbol{Q} = \begin{bmatrix} (0.025\ \text{m/s}^2)^2 & 0 & 0 \\ 0 & (0.1\,\text{deg/s})^2 & 0 \\ 0 & 0 & (0.1\,\text{deg/s})^2 \end{bmatrix} \tag{26}$$

The control effectiveness of the thrust is assumed to be uniformly distributed as

$$T_a = (1 + \Delta_T)T_c \tag{27}$$

where T_c and T_a are the command and actual thrust, respectively. The uncertainty Δ_T is uniformly distributed over $[-0.05, 0.05]$. The measurement noise in a typical speed indicator ΔV is assumed to be a Gaussian having a zero mean and 0.05 m/s ($\approx \pm 0.1$ kt) variance. Furthermore, a zero mean and 0.1-deg-variance Gaussian noise is assumed for both the flight-path angle $\Delta\gamma$ and the heading angle $\Delta\chi$ measurements.

C. Nonlinear Robust Control Design

Rewrite the dynamics of the selected UAV [Eq. (21)] in terms of Eq. (1) as

$$\dot{\boldsymbol{x}} = \boldsymbol{f}(\boldsymbol{x}) + \boldsymbol{B}(\boldsymbol{x})\boldsymbol{u} + \boldsymbol{G}\boldsymbol{w}, \qquad \boldsymbol{y} = \boldsymbol{x} \tag{28}$$

where

$$\boldsymbol{f}(\boldsymbol{x}) = \begin{bmatrix} -g\sin\gamma - gD_{\text{drag}}/W \\ -(g/V)\cos\gamma \\ 0 \end{bmatrix} \tag{29}$$

and

$$\boldsymbol{B}(\boldsymbol{x}) = \begin{bmatrix} g/W & 0 & 0 \\ 0 & k_n g/V & 0 \\ 0 & 0 & g k_n/(V\cos\gamma) \end{bmatrix} \tag{30}$$

To handle the nonaffine issue, a set of new control variables $\boldsymbol{u} \in \Re^{3\times 1}$ is introduced as $u_1 \triangleq T$, $u_2 \triangleq n_g\cos\phi$, and $u_3 \triangleq n_g\sin\phi$. Reversely, the actual control commands can be calculated by $\tan\phi = u_3/u_2$ and $n_g = \sqrt{u_2^2 + u_3^2}$.

The nominal model used in the robust stochastic control design is

$$\dot{\boldsymbol{x}} = \hat{\boldsymbol{f}}(\boldsymbol{x}) + \hat{\boldsymbol{B}}(\boldsymbol{x})\boldsymbol{u} \tag{31}$$

where

$$\hat{\boldsymbol{f}}(\boldsymbol{x}) = \begin{bmatrix} -g\sin\hat{\gamma} - g\hat{D}_{\text{drag},1}/W \\ -(g/\hat{V})\cos\hat{\gamma} \\ 0 \end{bmatrix} \tag{32}$$

and

$$\hat{\boldsymbol{B}}(\boldsymbol{x}) = \begin{bmatrix} g/W & 0 & 0 \\ 0 & k_n g/\hat{V} & 0 \\ 0 & 0 & gk_n/(\hat{V}\cos\hat{\gamma}) \end{bmatrix} \tag{33}$$

in which $\hat{D}_{\text{drag},1} = 0.5\rho\hat{V}^2 SC_{D0}$. The remaining part of the drag will be regarded as an uncertainty.

Based upon Theorem 2, the nonlinear robust control has the following form:

$$\boldsymbol{u} = \hat{\boldsymbol{B}}^{-1}\left[\frac{d\boldsymbol{y}_d}{dt} - \hat{\boldsymbol{f}}(\boldsymbol{x}) + \boldsymbol{\xi}\cdot\boldsymbol{s}\right] \tag{34}$$

and the sliding surface is $\boldsymbol{s} = \boldsymbol{y}_d - \boldsymbol{y}$, because the relative degree of the system is one [Eq. (18)]. To achieve the asymptotical stability, control parameters $\boldsymbol{\xi}$ need to satisfy

$$\boldsymbol{F} + \boldsymbol{D}\left|\frac{d\boldsymbol{y}_d}{dt} - \hat{\boldsymbol{f}}\right| + \boldsymbol{\eta}\cdot\boldsymbol{s} = (\boldsymbol{I} - \boldsymbol{D})\boldsymbol{\xi}\cdot\boldsymbol{s} \tag{35}$$

where $\boldsymbol{\eta} > 0$; $\boldsymbol{\eta} \in \Re^{3\times 1}$ will be selected through the optimization to be discussed in Sec. VI.D. Taking into account the uncertainties mentioned previously, the functional uncertainty bounds $\boldsymbol{F} = [F_1, F_2, F_3]^T$ are derived as

$$\begin{aligned} F_1 &= |\hat{f}_1 - f_1| = |g/W(D_{\text{drag},1} + D_{\text{drag},2} - \hat{D}_{\text{drag},1}) \\ &\quad + g\sin\gamma - g\sin\hat{\gamma}| \le g/W|D_{\text{drag},1} - \hat{D}_{\text{drag},1}| \\ &\quad + g/W|D_{\text{drag},2}| + g|\Delta\gamma| \end{aligned} \tag{36}$$

$$\begin{aligned} F_2 &= |\hat{f}_2 - f_2| = |(g/V)\cos\gamma \\ &\quad - (g/\hat{V})\cos\hat{\gamma}| \le (g/V_{\min})\Delta\gamma|\sin\gamma_{\max}| \end{aligned} \tag{37}$$

and $F_3 = 0$, where

$$\begin{aligned} &|(D_{\text{drag},1} - \hat{D}_{\text{drag},1})| = 0.5\rho SC_{D0}|(V - V_w)^2 - \hat{V}^2| \\ &\quad \le 0.5\rho SC_{D0}(\Delta V^2 + V_{w,\max}^2 + 2|V_{\max}(\hat{V} - V_w)_{\max}| \\ &\quad + 2|\Delta V V_{w,\max}|) \end{aligned} \tag{38}$$

and

$$|D_{\text{drag},2}| \le 2kk_n^2 W^2 n_{g,\max}^2/(\rho S|V_{\min} - V_{w,\max}|^2) \tag{39}$$

In the simulation, the speed of the UAV is assumed to be within 80–120 m/s, and the flight-path angle is constrained by ±10 deg. The uncertainty bounds of the input matrix $\boldsymbol{D} = \text{diag}[D_{11}, D_{22}, D_{33}]$ are derived as $D_{11} = 0.05$,

$$D_{22} = k_n g|(\hat{V} - V)/(V\hat{V})| \le k_n g(|\Delta V|)/V_{\min}^2 \tag{40}$$

and

$$\begin{aligned} D_{33} &= k_n g\left|\frac{1}{V\cos\gamma} - \frac{1}{\hat{V}\cos\hat{\gamma}}\right| \\ &\le k_n g\frac{|\Delta\gamma V_{\max}\sin\hat{\gamma} + \Delta V\Delta\gamma\sin\hat{\gamma}| + |\Delta V||\cos\hat{\gamma}|}{V_{\min}^2\cos^2\gamma_{\min}} \end{aligned} \tag{41}$$

when $\Delta\gamma$ is small.

D. Stochastic Control Design

With the control law defined as shown in Eqs. (34–41), the closed-loop system can be converted to the following Itô form as

$$d\widehat{\boldsymbol{x}} = \widehat{\boldsymbol{f}}(\boldsymbol{x},\boldsymbol{\eta})dt + \widehat{\boldsymbol{G}}d\boldsymbol{\beta}(t) \tag{42}$$

where

$$\widehat{\boldsymbol{f}}(\boldsymbol{x},\boldsymbol{\eta}) = [\widehat{f}_i]_{i=1,2,3} = \boldsymbol{f}(\boldsymbol{x}) + \boldsymbol{B}\hat{\boldsymbol{B}}^{-1}[d\boldsymbol{y}_d/dt - \hat{\boldsymbol{f}}(\boldsymbol{x}) + \boldsymbol{\xi}\cdot\boldsymbol{s}]$$

$\widehat{\boldsymbol{G}} = \boldsymbol{G}$, and $\boldsymbol{\xi}\cdot\boldsymbol{s}$ is a function of the control parameter $\boldsymbol{\eta} > 0$. Note that $d\boldsymbol{\beta}(t) \sim \boldsymbol{w}(t)dt$ and $\widehat{\boldsymbol{x}} = \boldsymbol{x}$ for this numerical example. The corresponding FPE that governs the state PDF $p(\widehat{\boldsymbol{x}})$ is derived as

$$\frac{\partial p}{\partial t} = -\sum_{i=1}^{3}\frac{\partial[p\widehat{f}_i]}{\partial\widehat{x}_i} + \sum_{i=1}^{3}\sum_{j=1}^{3}\frac{\partial^2[p(\boldsymbol{E}(\boldsymbol{x}))_{ij}]}{\partial\widehat{x}_i\partial\widehat{x}_j} \tag{43}$$

where $\boldsymbol{E} = \frac{1}{2}\widehat{\boldsymbol{G}}\boldsymbol{Q}\widehat{\boldsymbol{G}}^T$. In this example, the state PDF is approximated through the DQMOM approach as

$$p(\widehat{\boldsymbol{x}}) = \sum_{\alpha=1}^{N} w_\alpha(t)\prod_{j=1}^{3}\delta[\widehat{x}_j - \langle\widehat{x}_j\rangle_\alpha] \tag{44}$$

and the k_1, k_2, and k_3 moments of the state PDF are derived as

$$M^{k_1k_2k_3} = \sum_{\alpha=1}^{N} w_\alpha\prod_{j=1}^{3}\langle\widehat{x}_j\rangle_\alpha^{k_j} \tag{45}$$

E. Simulation Settings and Results

The moment constraints in Eq. (11) are selected to be

$$\begin{aligned} k_1 &= [1,0,0,2,0, \quad 0,1,1,0,3, \quad 0,0,2,2,0,1] \\ k_2 &= [0,1,0,0,2, \quad 0,1,0,1,0, \quad 3,0,1,0,2,2] \\ k_3 &= [0,0,1,0,0, \quad 2,0,1,1,0, \quad 0,3,0,1,1,0] \end{aligned} \tag{46}$$

for the case of $N = 4$ after trials and errors. In this moment description, for example, the first column $[1,0,0]^T$ gives the mean value of the speed, whereas the seventh column $[1,1,0]^T$ presents the covariance of the speed and the flight-path angle. The MATLAB® function `fminsearch` is used for the NLP optimization to find the proper control parameter $\boldsymbol{\eta}$. The Euler–Maruyama scheme [49] is used in the propagation of the SDE (42). The found control parameters are tested in 4000 Monte Carlo runs and compared with the case in which arbitrarily selected parameter $\boldsymbol{\eta} = [1,1,1]^T$ is used (i.e., without the offline stochastic optimization). To simplify the description, the proposed stochastic robust controller is denoted as method 1, and the nonlinear robust controller method using arbitrarily selected control parameters is represented as method 2. Note that the uncertainties and noise mentioned in Sec. VI.B are applied in the Monte Carlo simulation to show the robustness of the algorithm.

Of course, the control parameters can be carefully selected in method 2, but it may require many design iterations and intractable Monte Carlo simulations to obtain the desired statistics.

It can be seen in Figs. 2–7 that the mean values of the speed V, flight-path angle γ and heading angle χ are successfully controlled with relatively small steady-state errors in both methods, except in the speed histories in Figs. 2 and 3. Under these two different noises, the mean values of the speed achieved by method 1 are 89.64 and 89.45, respectively, whereas those of method 2 are 88.71 and 88.80, respectively. Therefore, in terms of controlling the mean value of the states, there are no significant differences between method 2 and the proposed method 1, because both methods are asymptotically stable in tracking.

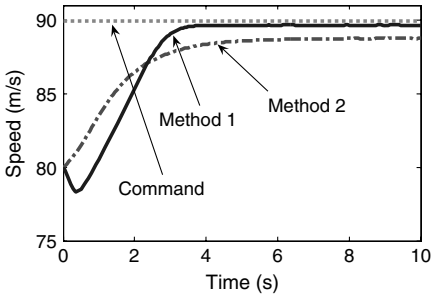

Fig. 2 Mean value of the speed (case 1).

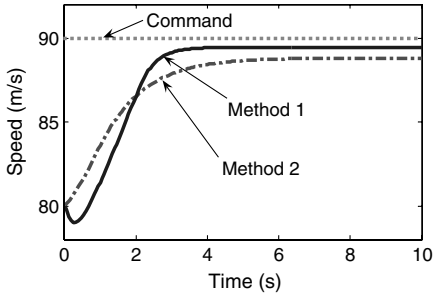

Fig. 3 Mean value of the speed (case 2).

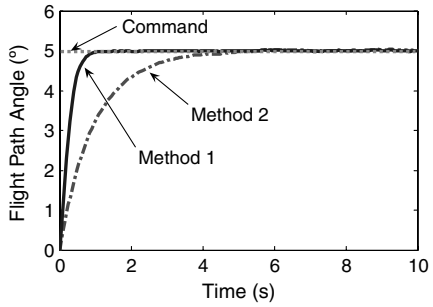

Fig. 4 Mean value of the flight-path angle (case 1).

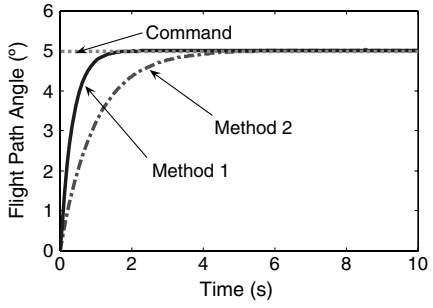

Fig. 5 Mean value of the flight-path angle (case 2).

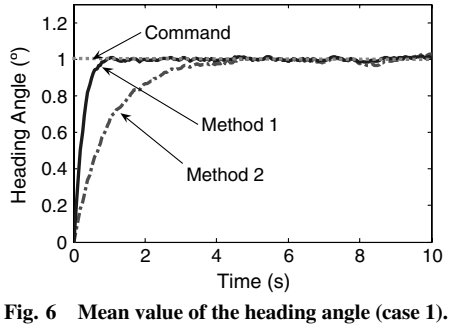

Fig. 6 Mean value of the heading angle (case 1).

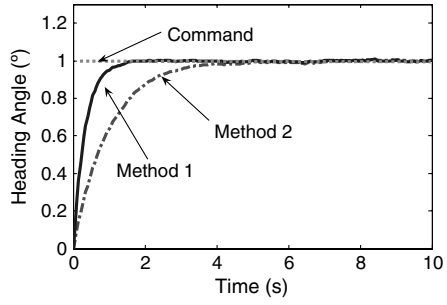

Fig. 7 Mean value of the heading angle (case 2).

The significance and advantage of method 1 can be easily seen from Figs. 8–11: method 1 has successfully controlled the variances $\sigma^2_{\dot{V},a}$, $\sigma^2_{\dot{\gamma},a}$, and $\sigma^2_{\dot{\chi},a}$ very closely toward the desired values as 0.095, 0.255, and 0.26 in case 1. Note that the units are intentionally neglected for a convenient description here. However, in method 2, the stationary variance values are 0.36 (Fig. 8), 1.04 (Fig. 10), and 1.05 (Fig. 10), respectively, which are far away from the desired statistic (0.1, 0.25, and 0.25, respectively). The same conclusion can be made in case 2, as shown in Figs. 9 and 11. Furthermore, as shown in Figs. 8 and 9, the relatively larger magnitude shown in the first part of speed variance represents a wider distribution of the speed

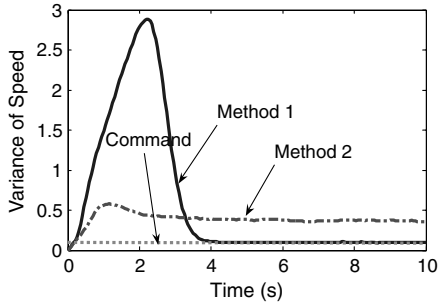

Fig. 8 Variance of the speed (case 1).

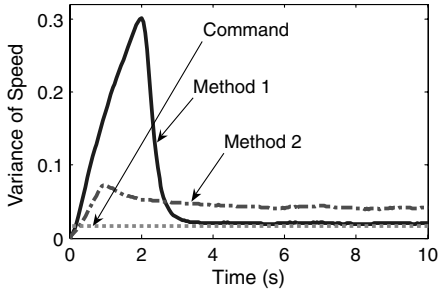

Fig. 9 Variance of the speed (case 2).

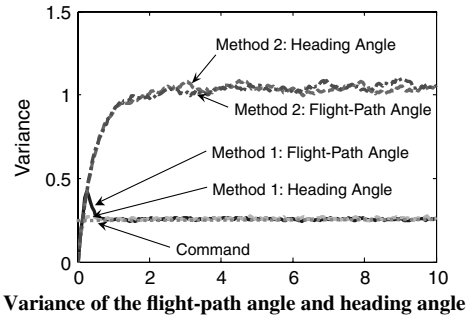

Fig. 10 Variance of the flight-path angle and heading angle (case 1).

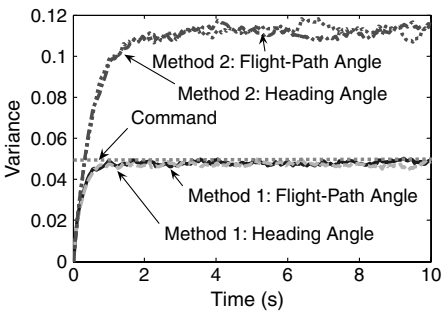

Fig. 11 Variance of the flight-path angle and heading angle (case 2).

Table 1 Stochastic control scenario and results: mean

Cases[a]	μ_V, m/s				μ_γ, deg				μ_χ, deg			
	$\mu_{V,d}$	$\mu_{V,o}$	$\mu_{V,a}$	$\mu_{V,t}$	$\mu_{\gamma,d}$	$\mu_{\gamma,o}$	$\mu_{\gamma,a}$	$\mu_{\gamma,t}$	$\mu_{\chi,d}$	$\mu_{\chi,o}$	$\mu_{\chi,a}$	$\mu_{\chi,t}$
1	90.000	90.000	89.650	88.710	5.000	5.000	5.000	5.020	1.000	1.000	1.000	0.990
2	90.000	90.000	89.450	88.800	5.000	4.990	5.000	5.000	1.000	1.000	1.000	0.990

[a]The control parameters are $\boldsymbol{\eta}_a = [4.239, 4.599, 4.500]^T$ for case 1 and $\boldsymbol{\eta}_a = [2.136, 2.798, 2.899]^T$ for case 2.

Table 2 Stochastic control scenario and results: variance

Cases[a]	σ_V^2, m^2/s^2				σ_γ^2, deg^2				σ_χ^2, deg^2			
	$\sigma_{V,d}^2$	$\sigma_{V,o}^2$	$\sigma_{V,a}^2$	$\sigma_{V,t}^2$	$\sigma_{\gamma,d}^2$	$\sigma_{\gamma,o}^2$	$\sigma_{\gamma,a}^2$	$\sigma_{\gamma,t}^2$	$\sigma_{\chi,d}^2$	$\sigma_{\chi,o}^2$	$\sigma_{\chi,a}^2$	$\sigma_{\chi,t}^2$
1	0.100	0.100	0.095	0.360	0.250	0.250	0.255	1.040	0.250	0.250	0.260	1.050
2	0.020	0.020	0.020	0.040	0.050	0.049	0.048	0.112	0.050	0.050	0.047	0.113

[a]The control parameters are $\boldsymbol{\eta}_a = [4.239, 4.599, 4.500]^T$ for case 1 and $\boldsymbol{\eta}_a = [2.136, 2.798, 2.899]^T$ for case 2.

performance in the Monte Carlo simulation, which does not mean a relatively larger transient performance.

In Tables 1 and 2, the subscripts d, o, a, and t denote the desired value, the value achieved from the offline optimization through the DQMOM approach, the actual value found in method 1 (validated through the Monte Carlo simulation), and the actual value found through method 2 (validated through the Monte Carlo simulation). The achieved control parameters $\boldsymbol{\eta}_a$ for both cases are listed as well. As shown, the stationary mean and variance values found from the optimization (method 1) match well with the Monte Carlo simulation. For example, the desired variance of the heading angle in case 1 is $\sigma_{\chi,d}^2 = 0.25$, the achieved variance in the optimization is $\sigma_{\chi,o}^2 = 0.25$, whereas when the control parameters obtained in the optimization is used in the Monte Carlo simulation, the achieved variance is $\sigma_{\chi,a}^2 = 0.26$. The same conclusion can be made for both cases.

Based on the theoretical derivation and simulation comparison, it can be concluded that the robust nonlinear control design satisfies the asymptotical stability under parametric and functional uncertainties, but they do not provide satisfactory in the statistical performance of the closed-loop system. By comparison, the method proposed here (i.e., method 1) provides a convenient and precise approach to quickly identify control parameters that enable the closed-loop system to have the desired statistical moment values.

VII. Conclusions

In this paper, a novel approach based upon the direct quadrature method of moments is proposed for nonlinear systems subject to parametric and functional uncertainties with random excitations. The state PDF in the closed-loop system is expressed in terms of a finite collection of Dirac delta functions, and the evolution of the associated weights and locations is governed by moment constraints. In this approach, the difficulties in solving the associated Fokker–Planck equation are alleviated. The proposed nonlinear feedback controller is robust with respect to parametric and functional uncertainties without discontinuous functions involved, which is preferred by the associated Fokker–Planck equation. The advantages of the method are as follows:

1) It is able to control the distribution of any specified stationary moments of the states/output probability density function.

2) The method is of interest because the process is not necessarily a Gaussian.

3) The controller is robust with respect to parametric and functional uncertainties without involving discontinuous functions.

A nontrivial UAV tracking problem has been used to demonstrate the capability of the proposed nonlinear stochastic control method.

Appendix A: Moments Equation in DQMOM

For convenience, the FPE of the state PDF [Eq. (9)] is repeated here as

$$\frac{\partial p}{\partial t} = -\sum_{i=1}^{N_s} \frac{\partial[p\widehat{f}_i]}{\partial \widehat{x}_i} + \frac{1}{2}\sum_{i=1}^{N_s}\sum_{j=1}^{N_s} \frac{\partial^2[p(\widehat{\boldsymbol{G}}\boldsymbol{Q}\widehat{\boldsymbol{G}}^T)_{ij}]}{\partial \widehat{x}_i \partial \widehat{x}_j} \tag{A1}$$

and the state PDF [50] can be represented as a summation of a multidimensional Dirac delta function:

$$p(\widehat{\boldsymbol{x}}(t)) = \sum_{\alpha=1}^{N} w_\alpha(t) \prod_{j=1}^{N_s} \delta[\widehat{x}_j - \langle \widehat{x}_j \rangle_\alpha(t)] \tag{A2}$$

Substituting Eq. (A2) into Eq. (A1), the LHS of Eq. (A1) is derived as

$$\begin{aligned}\frac{\partial p}{\partial t} &= \sum_{\alpha=1}^{N}\left(\frac{\partial w_\alpha}{\partial t}\right)\prod_{j=1}^{N_s}\delta[\widehat{x}_j - \langle \widehat{x}_j\rangle_\alpha] - \sum_{\alpha=1}^{N} w_\alpha \sum_{j=1}^{N_s}\prod_{q=1,q\neq j}^{N_s}\delta[\widehat{x}_q \\ &\quad - \langle \widehat{x}_q\rangle_\alpha]\frac{\partial \delta_{j\alpha}}{\partial \langle \widehat{x}_j\rangle_\alpha}\frac{\partial \langle \widehat{x}_j\rangle_\alpha}{\partial t} = \sum_{\alpha=1}^{N}\prod_{j=1}^{N_s}\delta_{j\alpha}\left(\frac{\partial w_\alpha}{\partial t}\right) \\ &\quad - \sum_{\alpha=1}^{N}\sum_{j=1}^{N_s}\prod_{q=1,q\neq j}^{N_s} w_\alpha \delta_{q\alpha}\delta'_{j\alpha}\frac{\partial \langle \widehat{x}_j\rangle_\alpha}{\partial t}\end{aligned} \tag{A3}$$

where $\delta_{j\alpha} \triangleq \delta[\widehat{x}_j - \langle \widehat{x}_j\rangle_\alpha]$ and $\delta'_{j\alpha} \triangleq \partial\delta_{j\alpha}/\partial\langle \widehat{x}_j\rangle_\alpha$. If the weighted abscissas $\zeta_{j\alpha} \triangleq w_\alpha \langle \widehat{x}_j\rangle_\alpha$ is introduced, Eq. (A3) can be further simplified as

$$\begin{aligned}\frac{\partial p}{\partial t} &= \sum_{\alpha=1}^{N}\left[\prod_{j=1}^{N_s}\delta_{j\alpha}\left(\frac{\partial w_\alpha}{\partial t}\right) + \sum_{j=1}^{N_s}\prod_{q=1,q\neq j}^{N_s}\langle \widehat{x}_j\rangle_\alpha \delta_{q\alpha}\delta'_{j\alpha}\frac{\partial w_\alpha}{\partial t}\right] \\ &\quad - \sum_{\alpha=1}^{N}\sum_{j=1}^{N_s}\prod_{q=1,q\neq j}^{N_s}\delta_{q\alpha}\delta'_{j\alpha}\frac{\partial \zeta_{j\alpha}}{\partial t}\end{aligned} \tag{A4}$$

Note that w_α, $\zeta_{j\alpha}$, and $\delta_{j\alpha}$ are functions of time, and thus the partial derivatives of the functions can be written as total derivatives:

$$\begin{aligned}\frac{\partial p}{\partial t} &= \sum_{\alpha=1}^{N}\left[\prod_{j=1}^{N_s}\delta_{j\alpha}\left(\frac{dw_\alpha}{dt}\right) + \sum_{j=1}^{N_s}\prod_{q=1,q\neq j}^{N_s}\langle \widehat{x}_j\rangle_\alpha \delta_{q\alpha}\delta'_{j\alpha}\frac{dw_\alpha}{dt}\right] \\ &\quad - \sum_{\alpha=1}^{N}\sum_{j=1}^{N_s}\prod_{q=1,q\neq j}^{N_s}\delta_{q\alpha}\delta'_{j\alpha}\frac{d\zeta_{j\alpha}}{dt}\end{aligned} \tag{A5}$$

With the definitions of

$$dw_\alpha/dt \triangleq a_\alpha, \qquad \alpha = 1, \ldots, N \tag{A6}$$

and

$$d\zeta_{j\alpha}/dt \triangleq c_{j\alpha}, \qquad j = 1, \ldots, N_s, \qquad \alpha = 1, \ldots, N \tag{A7}$$

Equation (A5) can be derived as

$$\frac{\partial p}{\partial t} = \sum_{\alpha=1}^{N}\left[\prod_{j=1}^{N_s}\delta_{j\alpha} + \sum_{j=1}^{N_s}\prod_{q=1,q\neq j}^{N_s}\langle\widehat{x}_j\rangle_\alpha\delta_{q\alpha}\delta'_{j\alpha}\right]a_\alpha - \sum_{\alpha=1}^{N}\left[\sum_{j=1}^{N_s}\prod_{q=1,q\neq j}^{N_s}\delta_{q\alpha}\delta'_{j\alpha}\right]c_{j\alpha} \tag{A8}$$

and the FPE can be written in terms of the multivariable Dirac delta function as

$$\sum_{\alpha=1}^{N}\left(\prod_{j=1}^{N_s}\delta_{j\alpha}\right)a_\alpha + \sum_{\alpha=1}^{N}\sum_{j=1}^{N_s}\prod_{q=1,q\neq j}^{N_s}\langle\widehat{x}_j\rangle_\alpha\delta_{q\alpha}\delta'_{j\alpha}a_\alpha - \sum_{\alpha=1}^{N}\left[\sum_{j=1}^{N_s}\prod_{q=1,q\neq j}^{N_s}\delta_{q\alpha}\delta'_{j\alpha}\right]c_{j\alpha} = S_x(\widehat{\boldsymbol{x}}) \tag{A9}$$

where the RHS of Eq. (A9) is denoted by the following expression:

$$S_x(\widehat{\boldsymbol{x}}) = -\sum_{i=1}^{N_s}\frac{\partial\widehat{pf}_i}{\partial\widehat{x}_i} + \sum_{i=1}^{N_s}\sum_{j=1}^{N_s}\frac{\partial^2[1/2\,\widehat{p(\boldsymbol{GQG}^T)}_{ij}]}{\partial\widehat{x}_i\partial\widehat{x}_j} \tag{A10}$$

It can be seen in Eq. (A9) that there are total $N(1+N_s)$ parameters to be found to construct the state PDF $p(\widehat{\boldsymbol{x}}(t))$: a_α and $c_{j\alpha}$ ($j=1,\ldots,N_s$ and $\alpha=1,\ldots,N$). The DQMOM method applies an independent set of user-defined moment constraints to construct $N(1+N_s)$ algebraic ODEs.

Given the following three Dirac delta function properties,

$$\int_{-\infty}^{+\infty}\widehat{x}^k\delta(\widehat{x}-\langle\widehat{x}\rangle_\alpha)\mathrm{d}\widehat{x} = \langle\widehat{x}\rangle_\alpha^k \tag{A11}$$

$$\int_{-\infty}^{+\infty}\widehat{x}^k\delta'(\widehat{x}-\langle\widehat{x}\rangle_\alpha)\mathrm{d}\widehat{x} = -k\langle\widehat{x}\rangle_\alpha^{k-1} \tag{A12}$$

and

$$\int_{-\infty}^{+\infty}\widehat{x}^k\delta''(\widehat{x}-\langle\widehat{x}\rangle_\alpha)\mathrm{d}\widehat{x} = k(k-1)\langle\widehat{x}\rangle_\alpha^{k-2} \tag{A13}$$

the $k_1, k_2, \ldots, k_{N_s}$ moments of Eq. (A9) can be written as follows:

$$\begin{aligned}&\int_{-\infty}^{+\infty}\cdots\int_{-\infty}^{+\infty}\widehat{x}_1^{k_1}\cdots\widehat{x}_{N_s}^{k_{N_s}}\left(\sum_{\alpha=1}^{N}\prod_{j=1}^{N_s}\delta_{j\alpha}a_\alpha\right)\prod_{l=1}^{N_s}\mathrm{d}\widehat{x}_l\\ &+\int_{-\infty}^{+\infty}\cdots\int_{-\infty}^{+\infty}\widehat{x}_1^{k_1}\cdots\widehat{x}_{N_s}^{k_{N_s}}\left(\sum_{\alpha=1}^{N}\sum_{j=1}^{N_s}\prod_{q=1,q\neq j}^{N_s}\langle\widehat{x}_j\rangle_\alpha\delta_{q\alpha}\delta'_{j\alpha}a_\alpha\right)\prod_{l=1}^{N_s}\mathrm{d}\widehat{x}_l\\ &-\int_{-\infty}^{+\infty}\cdots\int_{-\infty}^{+\infty}\widehat{x}_1^{k_1}\cdots\widehat{x}_{N_s}^{k_{N_s}}\left(\sum_{\alpha=1}^{N}\left[\sum_{j=1}^{N_s}\prod_{q=1,q\neq j}^{N_s}\delta_{q\alpha}\delta'_{j\alpha}\right]c_{j\alpha}\right)\prod_{l=1}^{N_s}\mathrm{d}\widehat{x}_l\\ &=\int_{-\infty}^{+\infty}\cdots\int_{-\infty}^{+\infty}\widehat{x}_1^{k_1}\cdots\widehat{x}_{N_s}^{k_{N_s}}[S_{\mathbf{x}}(\widehat{\boldsymbol{x}})]\prod_{l=1}^{N_s}\mathrm{d}\widehat{x}_l\end{aligned} \tag{A14}$$

After rearranging and simplifying Eq. (A14), the $N(1+N_s)$ unknown parameters can be found in

$$\sum_{\alpha=1}^{N}\left[\left(1-\sum_{j=1}^{N_s}k_j\right)\prod_{q=1}^{N_s}\langle\widehat{x}_q\rangle_\alpha^{k_q}\right]a_\alpha + \sum_{\alpha=1}^{N}\sum_{j=1}^{N_s}k_j\langle\widehat{x}_j\rangle_\alpha^{k_j-1}\prod_{q=1,q\neq j}^{N_s}\langle\widehat{x}_q\rangle_\alpha^{k_q}c_{j\alpha} = \bar{S}_{k_1,\ldots,k_{N_s}} \tag{A15}$$

where $\bar{S}_{k_1,\ldots,k_{N_s}} \triangleq \bar{S}^1_{k_1,\ldots,k_{N_s}} + \bar{S}^2_{k_1,\ldots,k_{N_s}}$. The first term in the LHS of Eq. (A15) can be simplified as

$$\int_{-\infty}^{+\infty}\cdots\int_{-\infty}^{+\infty}\widehat{x}_1^{k_1}\cdots\widehat{x}_{N_s}^{k_{N_s}}\left(\sum_{\alpha=1}^{N}\prod_{j=1}^{N_s}\delta_{j\alpha}a_\alpha\right)\mathrm{d}\widehat{x}_1\cdots\mathrm{d}\widehat{x}_{N_s} = \sum_{\alpha=1}^{N}\left(\prod_{j=1}^{N_s}\langle\widehat{x}_j\rangle_\alpha^{k_j}\right)a_\alpha \tag{A16}$$

whereas the second term in the LHS of Eq. (A15) is

$$\int_{-\infty}^{+\infty}\cdots\int_{-\infty}^{+\infty}\prod_{m=1}^{N_s}\widehat{x}_m^{k_m}\left(\sum_{\alpha=1}^{N}\sum_{j=1}^{N_s}\prod_{q=1,q\neq j}^{N_s}\langle\widehat{x}_j\rangle_\alpha\delta_{q\alpha}\delta'_{j\alpha}a_\alpha\right)\mathrm{d}\widehat{x}_1\cdots\mathrm{d}\widehat{x}_{N_s} = -\sum_{\alpha=1}^{N}\left(\sum_{j=1}^{N_s}k_j\prod_{q=1}^{N_s}\langle\widehat{x}_q\rangle_\alpha^{k_q}\right)a_\alpha \tag{A17}$$

In the same way, the third term of the LHS in Eq. (A15) is

$$-\sum_{\alpha=1}^{N}\sum_{j=1}^{N_s}c_{j\alpha}\int_{-\infty}^{+\infty}\widehat{x}_1^{k_1}\cdots\widehat{x}_{N_s}^{k_{N_s}}\delta'_{j\alpha}\left(\prod_{q=1,q\neq j}^{N_s}\delta_{q\alpha}\right)\mathrm{d}\widehat{x}_1\cdots\mathrm{d}\widehat{x}_{N_s} = \sum_{\alpha=1}^{N}\sum_{j=1}^{N_s}k_j\langle\widehat{x}_j\rangle_\alpha^{k_j-1}\prod_{q=1,q\neq j}^{N_s}\langle\widehat{x}_q\rangle_\alpha^{k_q}c_{j\alpha} \tag{A18}$$

The $k_1, k_2, \ldots, k_{N_s}$ moments of the RHS of Eq. (A15) are then derived to be

$$\begin{aligned}\bar{S}_{k_1,\ldots,k_{N_s}} &\triangleq \int_{-\infty}^{+\infty}\cdots\int_{-\infty}^{+\infty}\widehat{x}_1^{k_1}\cdots\widehat{x}_{N_s}^{k_{N_s}}S_{\mathbf{x}}(\widehat{\boldsymbol{x}})\mathrm{d}\widehat{x}_1\cdots\mathrm{d}\widehat{x}_{N_s}\\ &= -\sum_{i=1}^{N_s}\int_{-\infty}^{\infty}\widehat{x}_1^{k_1}\cdots\widehat{x}_{N_s}^{k_{N_s}}\frac{\partial[\widehat{pf}_i]}{\partial\widehat{x}_i}\mathrm{d}\widehat{x}_1\ldots\mathrm{d}\widehat{x}_{N_s}\\ &\quad+\int_{-\infty}^{\infty}\widehat{x}_1^{k_1}\cdots\widehat{x}_{N_s}^{k_{N_s}}\left[\sum_{i=1}^{N_s}\sum_{j=1}^{N_s}\frac{1}{2}\frac{\partial^2[\widehat{p(\boldsymbol{GQG}^T)}_{ij}]}{\partial\widehat{x}_i\partial\widehat{x}_j}\right]\mathrm{d}\widehat{x}_1\cdots\mathrm{d}\widehat{x}_{N_s}\\ &= \bar{S}^1_{k_1,\ldots,k_{N_s}} + \bar{S}^2_{k_1,\ldots,k_{N_s}}\end{aligned} \tag{A19}$$

where

$$\begin{aligned}\bar{S}^1_{k_1,\ldots,k_{N_s}} &= -\sum_{i=1}^{N_s}\int_{-\infty}^{\infty}\widehat{x}_1^{k_1}\cdots\widehat{x}_{N_s}^{k_{N_s}}\left(\frac{\partial\widehat{pf}_i}{\partial\widehat{x}_i}\right)\mathrm{d}\widehat{x}_1\cdots\mathrm{d}\widehat{x}_{N_s}\\ &= -\sum_{i=1}^{N_s}\int_{-\infty}^{\infty}\widehat{x}_1^{k_1}\cdots\widehat{x}_{N_s}^{k_{N_s}}\frac{\partial}{\partial\widehat{x}_i}\Big(\widehat{f}_i(\langle\widehat{x}_1\rangle_\alpha,\ldots\\ &\quad\langle\widehat{x}_{N_s}\rangle_\alpha)\sum_{\alpha=1}^{N}w_\alpha(t)\prod_{j=1}^{N_s}\delta_j\Big)\mathrm{d}\widehat{x}_1\cdots\mathrm{d}\widehat{x}_{N_s}\\ &= -\sum_{i=1}^{N_s}\sum_{\alpha=1}^{N}w_\alpha(t)\int_{-\infty}^{\infty}\widehat{x}_1^{k_1}\cdots\widehat{x}_{i-1}^{k_{i-1}}\widehat{x}_{i+1}^{k_{i+1}}\cdots\\ &\quad\widehat{x}_{N_s}^{k_{N_s}}\left(\int_{-\infty}^{\infty}\widehat{x}_i^{k_i}\frac{\partial}{\partial\widehat{x}_i}\left(\widehat{f}_i\prod_{j=1}^{N_s}\delta_j\right)\mathrm{d}\widehat{x}_i\right)\cdot\mathrm{d}\widehat{x}_1\cdots\mathrm{d}\widehat{x}_{i-1}\mathrm{d}\widehat{x}_{i+1}\cdots\mathrm{d}\widehat{x}_{N_s}\\ &= \sum_{i=1}^{N_s}\sum_{\alpha=1}^{N}k_iw_\alpha(t)\int_{-\infty}^{\infty}\widehat{x}_1^{k_1}\cdots\widehat{x}_{i-1}^{k_{i-1}}\widehat{x}_i^{k_i-1}\widehat{x}_{i+1}^{k_{i+1}}\cdots\\ &\quad\widehat{x}_{N_s}^{k_{N_s}}\widehat{f}\prod_{j=1}^{N_s}\delta_j\mathrm{d}\widehat{x}_1\cdots\mathrm{d}\widehat{x}_{i-1}\mathrm{d}\widehat{x}_i\mathrm{d}\widehat{x}_{i+1}\cdots\mathrm{d}\widehat{x}_{N_s}\\ &= \sum_{i=1}^{N_s}\sum_{\alpha=1}^{N}k_iw_\alpha(t)\langle\widehat{x}_1\rangle_\alpha^{k_1}\cdots\langle\widehat{x}_{i-1}\rangle_\alpha^{k_{i-1}}\langle\widehat{x}_i\rangle_\alpha^{k_i-1}\langle\widehat{x}_{i+1}\rangle_\alpha^{k_{i+1}}\cdots\\ &\quad\langle\widehat{x}_{N_s}\rangle_\alpha^{k_{N_s}}\widehat{f}_i(\langle\widehat{x}_1\rangle_\alpha,\cdots\langle\widehat{x}_{N_s}\rangle_\alpha)\end{aligned} \tag{A20}$$

Through a similar derivation, when $i\neq j$,

$$\bar{S}^2_{k_1,\ldots,k_{N_s}} = \int_{-\infty}^{\infty} \widehat{x}_1^{k_1} \cdots \widehat{x}_{N_s}^{k_{N_s}} \left[\sum_{i=1}^{N_s} \sum_{j=1}^{N_s} \frac{1}{2} \frac{\partial^2 [p(\widehat{\boldsymbol{G}}\boldsymbol{Q}\widehat{\boldsymbol{G}}^T)_{ij}]}{\partial \widehat{x}_i \partial \widehat{x}_j} \mathrm{d}\widehat{x}_1 \cdots \mathrm{d}\widehat{x}_{N_s} \right.$$
$$= \sum_{i=1}^{N_s} \sum_{j=1}^{N_s} \sum_{\alpha=1}^{N} w_\alpha k_i k_j \left(\prod_{q=1}^{N_s} \langle \widehat{x}_q \rangle_\alpha^{k_q} \right)$$
$$\left. \Big/ \langle \widehat{x}_i \rangle_\alpha \langle \widehat{x}_j \rangle_\alpha [\boldsymbol{E}(\widehat{\boldsymbol{x}})]_{ij} \right|_{\langle \widehat{x}_1 \rangle_\alpha, \ldots, \langle \widehat{x}_{N_s} \rangle_\alpha} \tag{A21}$$

whereas when $i = j$,

$$\bar{S}^2_{k_1,\ldots,k_{N_s}} = \int_{-\infty}^{\infty} \widehat{x}_1^{k_1} \cdots \widehat{x}_{N_s}^{k_{N_s}} \frac{\partial^2 f[\boldsymbol{E}(\widehat{\boldsymbol{x}})]_{ii}}{\partial \widehat{x}_i^2} \mathrm{d}\widehat{x}_1 \cdots \mathrm{d}\widehat{x}_{N_s}$$
$$= \sum_{i=1}^{N_s} \sum_{i=1}^{N_s} \sum_{\alpha=1}^{N} w_\alpha k_i (k_i - 1) \left(\prod_{q=1}^{N_s} \langle \widehat{x}_q \rangle_\alpha^{k_q} \right)$$
$$\Big/ \langle \widehat{x}_i \rangle_\alpha^2 [\boldsymbol{E}(\widehat{\boldsymbol{x}})]_{ii} |_{\langle \widehat{x}_1 \rangle_\alpha, \ldots, \langle \widehat{x}_{N_s} \rangle_\alpha} \tag{A22}$$

Thus, the $N(1 + N_s)$ ODEs can be constructed using a set of independent moment constraints $k_1, \ldots, k_{N_s}$, as shown in Eq. (11).

Appendix B: Stability Analysis of the Robust Nonlinear Control

To help illustrate the derivation, the sliding manifold in Eq. (18) is repeated here as

$$s_i = \sum_{k=0}^{r_i - 2} \lambda_{k,i} e_i^{(k)} + e_i^{(r_i - 1)}, \qquad i = 1, \ldots, p \tag{B1}$$

and $V = \boldsymbol{s}^T \boldsymbol{s}/2 \geq 0$ is chosen as the candidate Lyapunov function. Then the derivative of the sliding manifold can be written as

$$\dot{s}_i = \frac{d^{r_i} y_{i,d}}{dt^{r_i}} - \frac{d^{r_i} y_i}{dt^{r_i}} + \sum_{k=0}^{r_i - 2} \lambda_{k,i} e_i^{(k+1)}, \qquad i = 1, \ldots, p \tag{B2}$$

Using the matching condition, Eq. (B2) can be deduced in the vector form as

$$\dot{\boldsymbol{s}} = \frac{d^r \boldsymbol{y}_d}{dt^r} - L_f^r \boldsymbol{h}(\boldsymbol{x}) - L_{\boldsymbol{B}} L_f^{r-1} \boldsymbol{h}(\boldsymbol{x}) \boldsymbol{u} + \sum_{k=0}^{r-2} \boldsymbol{\lambda}_k \cdot \frac{d^{k+1} \boldsymbol{e}}{dt^{k+1}}$$
$$= \frac{d^r \boldsymbol{y}_d}{dt^r} - L_f^r \boldsymbol{h}(\boldsymbol{x}) - (\boldsymbol{I} + \boldsymbol{\Delta}) \left[\frac{d^r \boldsymbol{y}_d}{dt^r} - L_f^r \hat{\boldsymbol{h}}(\boldsymbol{x}) \right.$$
$$\left. + \sum_{k=o}^{r-2} \boldsymbol{\lambda}_k \cdot \boldsymbol{e}^{(k+1)} + \boldsymbol{\xi} \cdot \boldsymbol{s} \right] + \sum_{k=o}^{r-2} \boldsymbol{\lambda}_k \cdot \frac{d^{k+1} \boldsymbol{e}}{dt^{k+1}} = -L_{\hat{f}}^r \boldsymbol{h}(\boldsymbol{x})$$
$$+ L_{\hat{f}}^r \hat{\boldsymbol{h}}(\boldsymbol{x}) - \boldsymbol{\xi} \cdot \boldsymbol{s} - \boldsymbol{\Delta} \left[\frac{d^r \boldsymbol{y}_d}{dt^r} - L_f^r \hat{\boldsymbol{h}}(\boldsymbol{x}) + \sum_{k=o}^{r-2} \boldsymbol{\lambda}_k \cdot \boldsymbol{e}^{(k+1)} + \boldsymbol{\xi} \cdot \boldsymbol{s} \right]$$
$$\leq \boldsymbol{F} - \boldsymbol{\xi} \cdot \boldsymbol{s} - \boldsymbol{\Delta} \left[\frac{d^r \boldsymbol{y}_d}{dt^r} - L_f^r \hat{\boldsymbol{h}}(\boldsymbol{x}) + \sum_{k=o}^{r-2} \boldsymbol{\lambda}_k \cdot \boldsymbol{e}^{(k+1)} + \boldsymbol{\xi} \cdot \boldsymbol{s} \right]$$
$$= \boldsymbol{F} - \boldsymbol{\xi} \cdot \boldsymbol{s} - \boldsymbol{\Delta} \boldsymbol{\xi} \cdot \boldsymbol{s} - \boldsymbol{\Delta} \frac{d^r \boldsymbol{y}_d}{dt^r} + \boldsymbol{\Delta} L_f^r \hat{\boldsymbol{h}}(\boldsymbol{x})$$
$$- \boldsymbol{\Delta} \sum_{k=o}^{r-2} \boldsymbol{\lambda}_k \cdot \boldsymbol{e}^{(k+1)} \leq \boldsymbol{F} - (\boldsymbol{I} - \boldsymbol{D}) \boldsymbol{\xi} \cdot \boldsymbol{s}$$
$$- \boldsymbol{\Delta} \left[\frac{d^r \boldsymbol{y}_d}{dt^r} - L_f^r \hat{\boldsymbol{h}}(\boldsymbol{x}) + \sum_{k=o}^{r-2} \boldsymbol{\lambda}_k \cdot \boldsymbol{e}^{(k+1)} \right] \leq \boldsymbol{F} - (\boldsymbol{I} - \boldsymbol{D}) \boldsymbol{\xi} \cdot \boldsymbol{s}$$
$$+ \boldsymbol{D} \left| \frac{d^r \boldsymbol{y}_d}{dt^r} - L_f^r \hat{\boldsymbol{h}}(\boldsymbol{x}) + \sum_{k=o}^{r-2} \boldsymbol{\lambda}_k \cdot \boldsymbol{e}^{(k+1)} \right| = -\boldsymbol{\eta} \cdot \boldsymbol{s} \tag{B3}$$

Here, $\boldsymbol{\eta} > 0$. Therefore, if $s_i \neq 0$, then $\dot{V} < 0$. In the case of $s_i = 0$,

$$e_i^{(r_i - 1)} = -\sum_{k=0}^{r_i - 2} \lambda_{k,i} e_i^{(k)}$$

Let us define $\boldsymbol{e}_i = [e_i, \dot{e}_i, \ldots, e_i^{r_i - 2}]^T$, and thus $\dot{\boldsymbol{e}}_i = [\dot{e}_i, \ddot{e}_i, \ldots, e_i^{r_i - 1}]^T = \boldsymbol{A} \boldsymbol{e}_i$, where

$$\boldsymbol{A} = \begin{bmatrix} 0 & 1 & 0 & \cdots & 0 \\ 0 & 0 & 1 & \cdots & 0 \\ \vdots & \vdots & \vdots & \vdots & \vdots \\ 0 & 0 & 0 & 0 & 1 \\ -\lambda_{0,i} & -\lambda_{1,i} & \cdots & \cdots & -\lambda_{r_i - 2,i} \end{bmatrix} \tag{B4}$$

With a properly chosen $\lambda_{k,i}$ $(k = 0, \ldots, r_i - 2)$, matrix $\boldsymbol{A}$ is a Hurwitz matrix and all the eigenvalues of $\boldsymbol{A}$ have strictly negative real parts. For any matrix $\boldsymbol{R} = \boldsymbol{R}^T > 0$, there is a unique solution that satisfies $\boldsymbol{P}\boldsymbol{A} + \boldsymbol{A}^T \boldsymbol{P} = -\boldsymbol{R}$ and $\boldsymbol{P} = \boldsymbol{P}^T > 0$. The derivative of the selected Lyapunov function $V_1 = \boldsymbol{e}^T \boldsymbol{P} \boldsymbol{e} \geq 0$ can be derived as

$$\dot{V}_1 = (\boldsymbol{A}\boldsymbol{e}_i)^T \boldsymbol{P} \boldsymbol{e} + \boldsymbol{e}^T \boldsymbol{P} \boldsymbol{A} \boldsymbol{e}_i = -\boldsymbol{e}_i^T \boldsymbol{R} \boldsymbol{e}_i \leq -\lambda_{\min}(\boldsymbol{R}) \|\boldsymbol{e}_i\|_2^2 \tag{B5}$$

where $\lambda_{\min}(\boldsymbol{R})$ is the minimum eigenvalue of the matrix $\boldsymbol{R}$.

Because the set $\{\dot{V}_1(\boldsymbol{e}_i) = 0\}$ contains no trajectory of the system except the trivial one $\boldsymbol{e}_i = 0$, the controlled system is globally asymptotically stable [51].

Appendix C: Proof of Lemma 1

Based on Eq. (B3), $\forall\, s_i > 0$, the Lyapunov stability requires

$$F_i + \sum_{j=1}^{p} D_{ij} |y_{j,d}^{r_j} - L_{\hat{f}}^{r_j} \hat{h}_j + \sum_{k=0}^{r_j - 2} \lambda_{k,j} e_j^{(k+1)}| + \eta_i s_i$$
$$= \xi_i s_i - \sum_{j=1}^{p} D_{ij} |\xi_i s_j| \tag{C1}$$

and $\forall\, s_i < 0$, the Lyapunov stability requires

$$F_i + \sum_{j=1}^{p} D_{ij} |y_{j,d}^{r_j} - L_{\hat{f}}^{r_j} \hat{h}_j + \sum_{k=0}^{r_j - 2} \lambda_{k,j} e_j^{(k+1)}| - \eta_i s_i$$
$$= -\xi_i s_i - \sum_{j=1}^{p} D_{ij} |\xi_i s_j| \tag{C2}$$

For case 1, $s_i > 0$ or $s_i < 0$, $\forall\, i \in [1, \ldots, p]$; under this case, both Eqs. (C1) and (C2) can be written as

$$F_i + \sum_{j=1}^{p} D_{ij} |y_{j,d}^{r_j} - L_{\hat{f}}^{r_j} \hat{h}_j + \sum_{k=0}^{r_j - 2} \lambda_{k,j} e_j^{(k+1)}| + |\eta_i s_i|$$
$$= |\xi_i s_i| - \sum_{j=1}^{p} D_{ij} |\xi_i s_j| \tag{C3}$$

Let us define $\kappa_i = |\xi_i s_i| > 0$ and $\boldsymbol{\kappa} = [\xi_1, \ldots, \xi_p] \in \Re^p$. Equation (C3) can be written in a vector form as

$$\boldsymbol{\zeta} = \boldsymbol{\kappa} - \boldsymbol{D}\boldsymbol{\kappa} = (\boldsymbol{I} - \boldsymbol{D})\boldsymbol{\kappa} \tag{C4}$$

where $\boldsymbol{\zeta} = [\zeta_i]$ $(i = 1, \ldots, p)$,

$$\zeta_i = F_i + \sum_{j=1}^{p} D_{ij} |y_{j,d}^{r_j} - L_{\hat{f}}^{r_j} \hat{h}_j + \sum_{k=0}^{r_j - 2} \lambda_{k,j} e_j^{(k+1)}| + |\eta_i s_i| \tag{C5}$$

Because of the uncertainty matching function [41], the maximum eigenvalue of matrix $\boldsymbol{D}$ is less than one. According to the Perron–Frobenius theorem, if $\boldsymbol{\zeta} > 0$ and the maximum eigenvalue of matrix $\boldsymbol{D}$ is less than one, there exists a unique solution of $\boldsymbol{\kappa}$ and $\boldsymbol{\kappa} > 0$. The unique and positive $\boldsymbol{\xi}$ can be found by

$$\xi_i = \begin{cases} \kappa_i / s_i & s_i > 0 \\ -\kappa_i / s_i & s_i < 0 \end{cases} \tag{C6}$$

For case 2, $s_l > 0$, $s_q < 0$, $l, q \in [1, \ldots, p]$, and $q \neq l$. Let us define $\kappa_l = \xi_l s_l$ for $s_l > 0$ and $\kappa_q = -\xi_q s_q$ for $s_q < 0$. Equations (C1) and (C2) can be simplified as

$$F_l + \sum_{j=1}^{p} D_{lj} \left| y_{j,d}^{r_j} - L_{\hat{f}}^{r_j} \hat{h}_j + \sum_{k=0}^{r_j - 2} \lambda_{k,j} e_j^{(k+1)} \right| + \eta_l s_l = \xi_l s_l - \sum_{j=1}^{p} D_{lj} |\xi_j s_j| \tag{C7}$$

and

$$F_q + \sum_{j=1}^{p} D_{qj} \left| y_{j,d}^{r_j} - L_{\hat{f}}^{r_j} \hat{h}_j + \sum_{k=0}^{r_j - 2} \lambda_{k,j} e_j^{(k+1)} \right| - \eta_q s_q = -\xi_q s_q - \sum_{j=1}^{p} D_{qj} |\xi_j s_j| \tag{C8}$$

The left sides of both Eqs. (C6) and (C7) are positive values. Using the preceding definition for $\boldsymbol{\zeta}$, the first term of the right side is also positive. Equations (C6) and (C7) can be written in the vector form as $\boldsymbol{\zeta} = (\boldsymbol{I} - \boldsymbol{D})\boldsymbol{\kappa}$. Based on the same derivation as shown in case 1, there exists a unique and positive solution for $\boldsymbol{\kappa}$, from which a unique $\boldsymbol{\xi}$ can be calculated explicitly. In case of $s_i \to 0$, the magnitude of $\xi_i s_i (\zeta_i = |\xi_i s_i|)$ instead of ξ_i will be calculated.

Acknowledgments

The author would like to thank Prakash Vedula for many helpful discussions regarding quadrature-based methods. The author gratefully acknowledges the reviewers and the Associate Editor for their suggestions.

References

[1] Wang, Q., and Stengel, R. F., "Probabilistic Control of Nonlinear Uncertain Systems," *Probabilistic and Randomized Methods for Design Under Uncertainty*, Springer–Verlag, London, 2006, pp. 381–414.

[2] Davis, M. H. A., and Vinter, R. B., *Stochastic Modeling and Control*, Chapman and Hall, London, 1985, p. 266.

[3] Oshman, Y., "Linear Quadratic Stochastic Control Using the Singular Value Decomposition," *Journal of Guidance, Control, and Dynamics*, Vol. 15, No. 4, 1992, pp. 1045–1047. doi:10.2514/3.20945

[4] Frangos, C., and Yavin, Y., "Feasible Controller Design for Stochastic Systems," *Journal of Guidance, Control, and Dynamics*, Vol. 20, No. 3, May–June 1997, pp. 535–541. doi:10.2514/2.4073

[5] Speyer, J. L., and Gustafson, D. E., "Stochastic Optimization Control of Linear Dynamic System," *AIAA Journal*, Vol. 12, No. 8, Aug. 1974, pp. 1013–1020. doi:10.2514/3.49403

[6] Iwasaki, T., and Skelton, R. E., "On the Observer-Based Structure of Covariance Controllers," *Systems and Control Letters*, Vol. 22, No. 1, 1994, pp. 17–25. doi:10.1016/0167-6911(94)90022-1

[7] Lewis, A. S., and Sinha, A., "Sliding Mode Control of Mechanical Systems with Bounded Disturbances via Output Feedback," *Journal of Guidance, Control, and Dynamics*, Vol. 22, No. 2, Mar.–Apr. 1999, pp. 235–240. doi:10.2514/2.4400

[8] Grigoriadis, K. M., and Skelton, R. E., "Minimum-Energy Covariance Controllers," *Automatica*, Vol. 33, No. 4, 1997, pp. 569–578. doi:10.1016/S0005-1098(96)00188-4

[9] Bratus, A., Dimentberg, M., and Iourtchenko, D., "Optimal Bounded Response Control for a Second-Order System Under a White-Noise Excitation," *Journal of Vibration and Control*, Vol. 6, No. 5, 2000, pp. 741–755. doi:10.1177/107754630000600506

[10] Hotz, A., and Skelton, R. E., "Covariance Control Theory," *International Journal of Control*, Vol. 46, No. 1, 1987, pp. 13–32. doi:10.1080/00207178708933880

[11] Hu, G., Lou, Y., and Christofides, P. D., "Dynamic Output Feedback Covariance Control of Linear Stochastic Dissipative Partial Differential Equations," *2008 American Control Conference*, Inst. of Electrical and Electronics Engineers, Piscataway, NJ, 11–13 June 2008, pp. 260–266.

[12] Lou, Y., and Christofides, P. D., "Nonlinear Feedback Control of Surface Roughness Using a Stochastic PDE," *45th IEEE Conference on Decision and Control*, Inst. of Electrical and Electronics Engineers, Piscataway, NJ, 13–15 Dec. 2006, pp. 936–943.

[13] Young, G. E., and Chang, R. J., "Optimal Control of Stochastic Parametrically and Externally Excited Nonlinear Control Systems," *Journal of Dynamic Systems, Measurement, and Control*, Vol. 110, No. 2, 1988, pp. 114–119.

[14] Wojtkiewicz, S. F., and Bergman, L. A., "A Moment Specification Algorithm for Control of Nonlinear System Driven by Gaussian White Noise," *Nonlinear Dynamics*, Vol. 24, No. 1, 2001, pp. 17–30. doi:10.1023/A:1026575320113

[15] Jazwinski, A., *Stochastic Processes and Filtering Theory*, Academic Press, New York, 1970; reprint, Academic Press, New York, 2007, pp. 72–74.

[16] Fokker, A., *Annalen der Physik*, Vol. 43, No. 810, 1940.

[17] Planck, M., "Sitzungsberichte der Königlich Preussischen Akademie der Wissenschaften," 1917, p. 324.

[18] Zhou, Y., and Chirikjian, G. S., "Probabilistic Models of Dead-Reckoning Error in Nonholonomic Mobile Robots," *Proceedings of IEEE International Conference on Robotics and Automation*, Vol. 2, Inst. of Electrical and Electronics Engineers, Piscataway, NJ, 2003, pp. 1594–1599.

[19] Spencer, B. F., Jr., and Bergman, L. A., "On the Numerical Solution of the Fokker Equations for Nonlinear Stochastic Systems," *Nonlinear Dynamics*, Vol. 4, No. 4, 1993, pp. 357–372. doi:10.1007/BF00120671

[20] Hexner, G., and Shima, T., "Stochastic Optimal Control Guidance Law with Bounded Acceleration," *IEEE Transactions on Aerospace and Electronic Systems*, Vol. 43, No. 1, Jan. 2007, pp. 71–77. doi:10.1109/TAES.2007.357155

[21] Daum, F., "Nonlinear Filters: Beyond the Kalman Filter," *IEEE Aerospace and Electronic Systems Magazine*, Vol. 20, No. 8, 2005, Part 2, pp. 57–69. doi:10.1109/MAES.2005.1499276

[22] Naess, A., and Johnson, J. M., "Response Statistics of Nonlinear Dynamics Systems by Path Integration," *Proceedings of IUTAM Symposium on Nonlinear Stochastic Mechanics*, edited by F. Casciati and N. Bellomo, Springer–Verlag, Berlin, 1992, pp. 401–414.

[23] Sun, J. Q., and Hsu, C. S., "The Generalized Cell Mapping Method in Nonlinear Random Vibration Based upon Short-Time Gaussian Approximation," *Journal of Applied Mechanics*, Vol. 57, No. 4, 1990, pp. 1018–1025. doi:10.1115/1.2897620

[24] Challa, S., and Bar-Shalom, Y., "Nonlinear Filter Design Using Fokker–Planck-Kolmogorov Probability Density Evolutions," *IEEE Transactions on Aerospace and Electronic Systems*, Vol. 36, No. 1, 2000, pp. 309–315. doi:10.1109/7.826335

[25] Yoon, J., and Xu, Y., "Relative Position Estimation Using Fokker–Planck and Bayes' Equations," 2007 AIAA Guidance, Control, and Dynamics Conference, Hilton Head, SC, AIAA Paper 2007-6658, 20–23 Aug. 2007.

[26] Sun, J. Q., and Hsu, C. S., "Cumulant-Neglect Closure Method for Asymmetric Nonlinear Systems Driven by Gaussian White Noise," *Journal of Sound and Vibration*, Vol. 135, No. 2, 1989, pp. 338–345. doi:10.1016/0022-460X(89)90730-X

[27] Sobczy, K., and Trebicki, J., "Maximum Entropy Principle in Stochastic Dynamics," *Probabilistic Engineering Mechanics*, Vol. 3, No. 5, 1990, pp. 102–110.

[28] Chang, K. Y., Wang, W. J., and Chang, W. J., "Constrained Control for Stochastic Multivariable Systems with Hysteresis Nonlinearity," *International Journal of Systems Science*, Vol. 28, No. 7, 1997, pp. 731–736. doi:10.1080/00207729708929432

[29] Kim, J., and Rock, S., "Stochastic Feedback Controller Design Considering the Dual Effect," AIAA Guidance, Navigation, and Control Conference and Exhibit, AIAA Paper 2006-6090, Keystone, CO, Aug. 2006.

[30] Forbes, M. G., Forbes, J. F., and Guay, M., "Regulatory Control Design for Stochastic Processes: Shaping the Probability Density Function,"

Proceedings of the American Control Conference, Inst. of Electrical and Electronics Engineers, Piscataway, NJ, 4–6 June 2003, pp. 3998–4003.

[31] Su, Q., and Strunz, K., "Stochastic Polynomial-Chaos-Based Average Model of Twelve-Pulse Diode Rectifier for Aircraft Applications," *2006 IEEE Workshop on Computers in Power Electronics (COMPEL 2006)*, Inst. of Electrical and Electronics Engineers, Piscataway, NJ, 16–19 July 2006, pp. 64–68.

[32] Sun, J. Q., and Xu, Q., "Response Variance Reduction of a Nonlinear Mechanical System via Sliding Mode Control," *Journal of Vibration and Acoustics*, Vol. 120, July 1998, pp. 801–805. doi:10.1115/1.2893900

[33] Yue, H., and Wang, H., "Minimum Entropy Control of Closed-Loop Tracking Errors for Dynamic Stochastic Systems," *IEEE Transactions on Automatic Control*, Vol. 48, No. 1, Jan. 2003, pp. 118–122. doi:10.1109/TAC.2002.806663

[34] Kumar, M., Chakravorty, S., and Junkins, J. L., "Computational Nonlinear Stochastic Control Based on the Fokker–Planck-Kolmogorov Equation," AIAA Guidance, Navigation, and Control Conference and Exhibit, AIAA Paper 2008-6477, Honolulu, HI, Aug. 2008.

[35] Utkin, V. I., "Variable Structure Systems with Sliding Modes," *IEEE Transactions on Automatic Control*, Vol. 22, No. 2, Apr. 1977, pp. 212–222. doi:10.1109/TAC.1977.1101446

[36] Bartolini, G., Punta, E., and Zolezzi, T., "Simplex Methods for Nonlinear Uncertain Sliding Mode Control," *IEEE Transactions on Automatic Control*, Vol. 49, No. 6, June 2004, pp. 922–933. doi:10.1109/TAC.2004.829617

[37] Hung, J. Y., Gao, W., and Hung, J. C., "Variable Structure Control: A Survey," *IEEE Transactions on Industrial Electronics*, Vol. 40, No. 1, Feb. 1993, pp. 2–22. doi:10.1109/41.184817

[38] Bartolini, G., Ferrara, A., Usai, E., and Utkin, V. I., "On Multi-Input Chattering-Free Second Order Sliding Mode Control," *IEEE Transactions on Automatic Control*, Vol. 45, No. 9, Sept. 2000, pp. 1711–1717. doi:10.1109/9.880629

[39] Perruquetti, W., and Barbot, J. P., *Sliding Mode Control in Engineering*, Marcel Dekker, New York, 2002, pp. 12–14.

[40] Lee, J. G., Park, C. G., and Park, H. W., "Sliding-Mode Controller Design for Spacecraft Attitude Tracking Maneuvers," *IEEE Transactions on Aerospace and Electronics Systems*, Vol. 29, No. 4, Oct. 1993, pp. 1328–1333. doi:10.1109/7.259536

[41] Slotine, J. E., and Li, W., *Applied Nonlinear Control*, Prentice–Hall, Upper Saddle River, NJ, 1990, pp. 267–307.

[42] Buffington, J. M., and Shtessel, Y. B., "Saturation Protection for Feedback Linearizable Systems Using Sliding Mode Theory," *Proceedings of the 1998 American Control Conference*, Inst. of Electrical and Electronics Engineers, Piscataway, NJ, 1998, pp. 1028–1032.

[43] Phuah, J., Lu, J., and Yahagi, T., "Chattering Free Sliding Mode Control in Magnetic Levitation System," *IEEJ Transactions on Electronics Information and Systems*, Vol. 125, Pt. 4, 2005, pp. 600–606. doi:10.1541/ieejeiss.125.600

[44] Yao, B., and Tomizuka, M., "Smooth Robust Adaptive Sliding Mode Control of Manipulators with Guaranteed Transient Performance," *Proceedings of the 1994 American Control Conference*, Inst. of Electrical and Electronics Engineers, Piscataway, NJ, 1994, pp. 1176–1180.

[45] Kokotovic, P., Khalil, H. K., and O'Reilly, J., *Singular Perturbation Methods in Control, Analysis and Design*, Society for Industrial and Applied Mathematics, Philadelphia, 1999, pp. 1–45.

[46] Hopkins, R., and Xu, Y., "Position Tracking Control for a Simulated Miniature Helicopter," 2008 AIAA Guidance, Navigation, and Control Conference and Exhibit, Honolulu, HI, AIAA Paper 2008-6485, 18–21 Aug. 2008.

[47] Unnikrishnam, N., and Balakrishnan, S. N., "Neuroadaptive Model Following Controller Design for a Nonaffine UAV Model," *Proceedings of the 2006 American Control Conference*, Inst. of Electrical and Electronics Engineers, Piscataway, NJ, 14–16 June 2006, pp. 2961–2956.

[48] "Advisory Circular," U.S. Department of Transportation and Federal Aviation Administration, Rept. AC 120-28D, July 1999, App. 4.

[49] Kloeden, P. E., and Platen, E., *Numerical Solution of Stochastic Differential Equations*, Springer–Verlag, Berlin, 1992, pp. 340–344.

[50] Marchisio, D. L., and Fox, R. O., "Solution of Population Balance Equations Using the Direct Quadrature Method of Moments" *Journal of Aerosol Science*, Vol. 36, No. 1, 2005, pp. 43–73. doi:10.1016/j.jaerosci.2004.07.009

[51] LaSalle, J. P., "Some Extensions of Lyapunov's Second Method," *IRE Transactions on Circuit Theory*, Vol. 7, No. 4, 1960, pp. 520–527.